LOW MASS STAR FORMATION

- Star formation: from spherical to axisymmetric
- Herbig-Haro flows and molecular outflows
- Disks and jets
- The case of L1551 IRS5

<1980

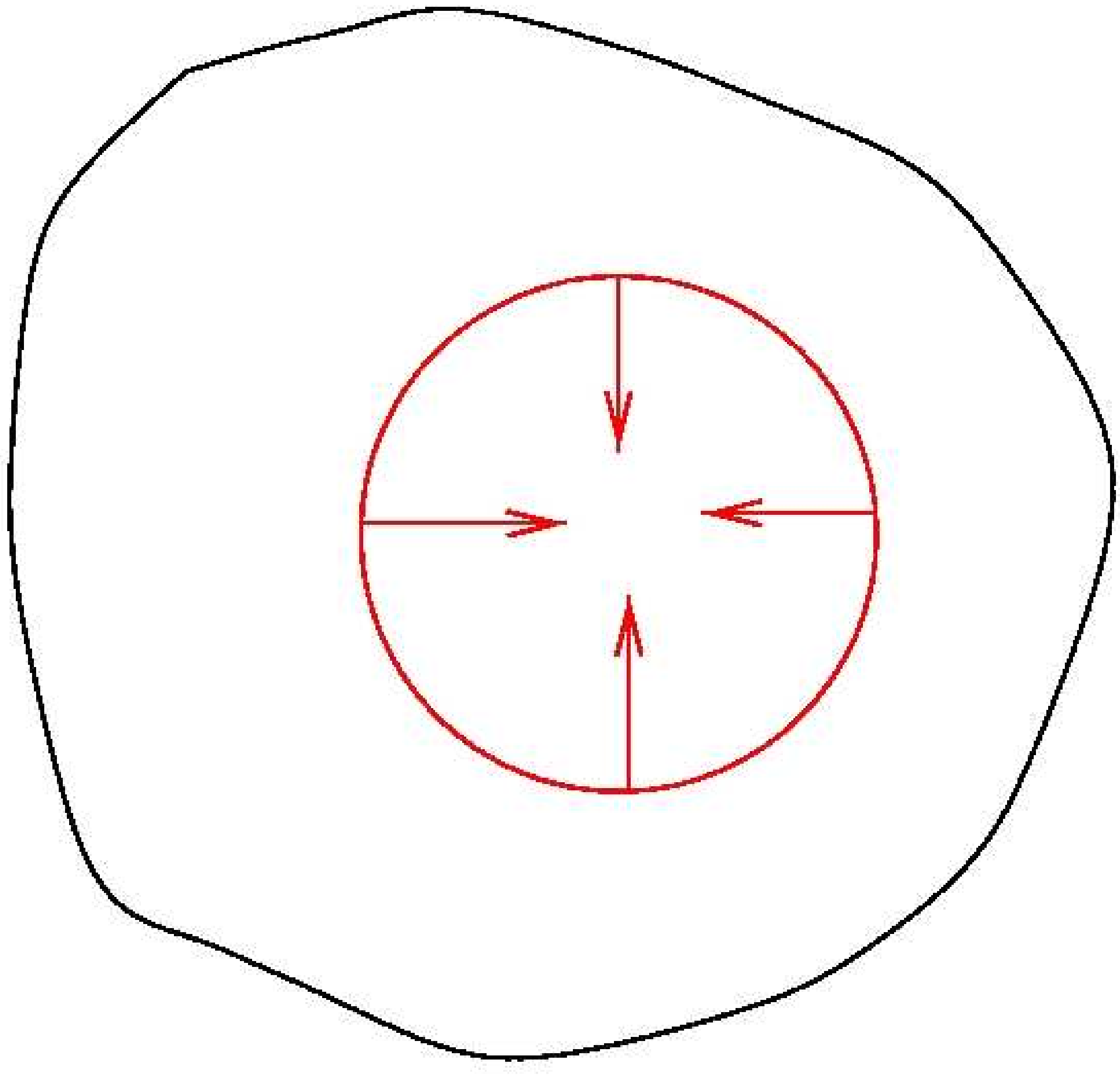

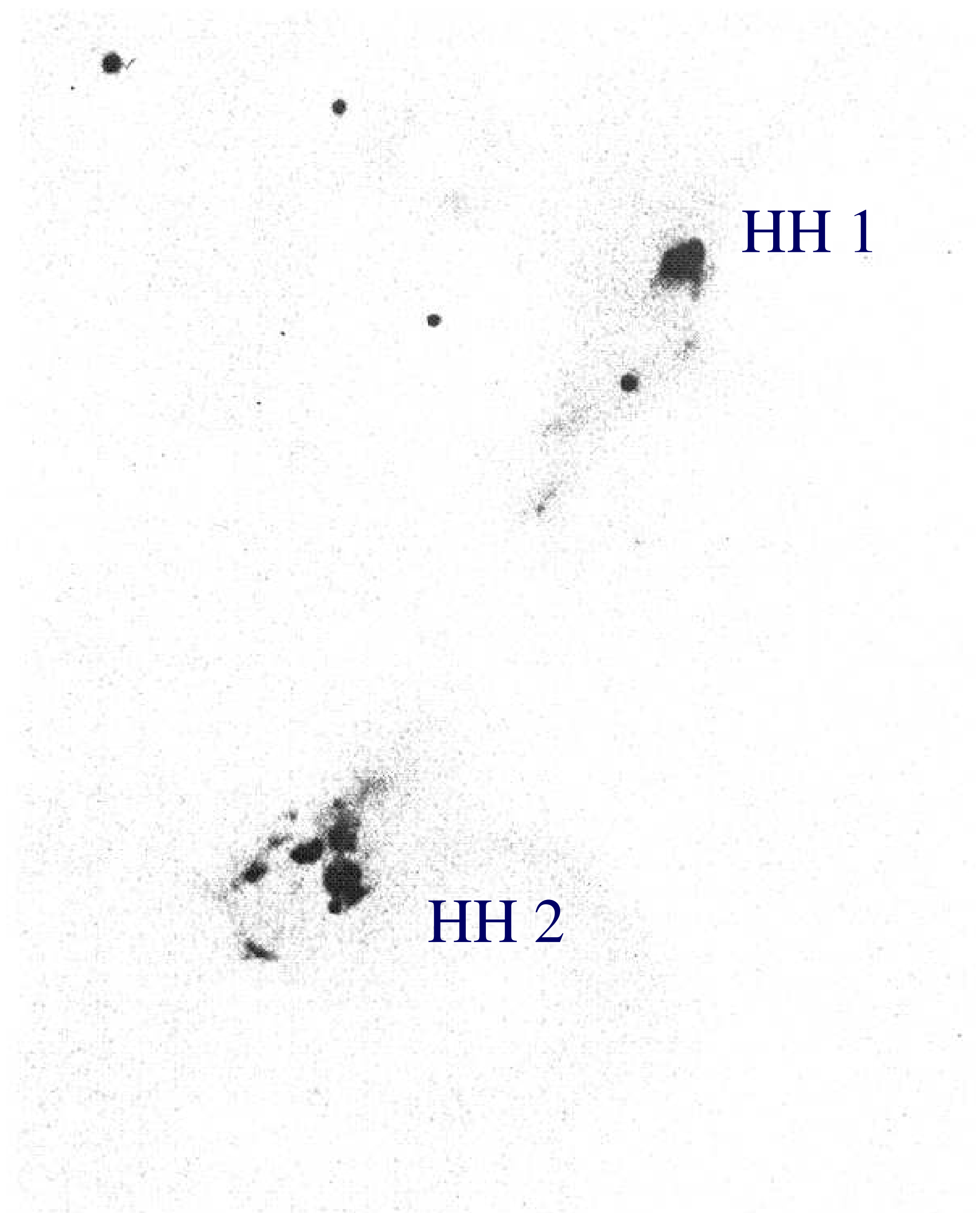

FIG. 3. Contrast-enhanced enlargement of the region of HH 1, HH 2, and the C-S star, from 120-in. plate ED-32; see Fig. 7 for identifications. The faint nebulosity centered on the C-S star is apparent, and its elongation in the directions of HH 1 and HH 2. The small ring of faint nebulosity to the upper left of HH 1, and the much larger ring to the right of HH 2 are real.

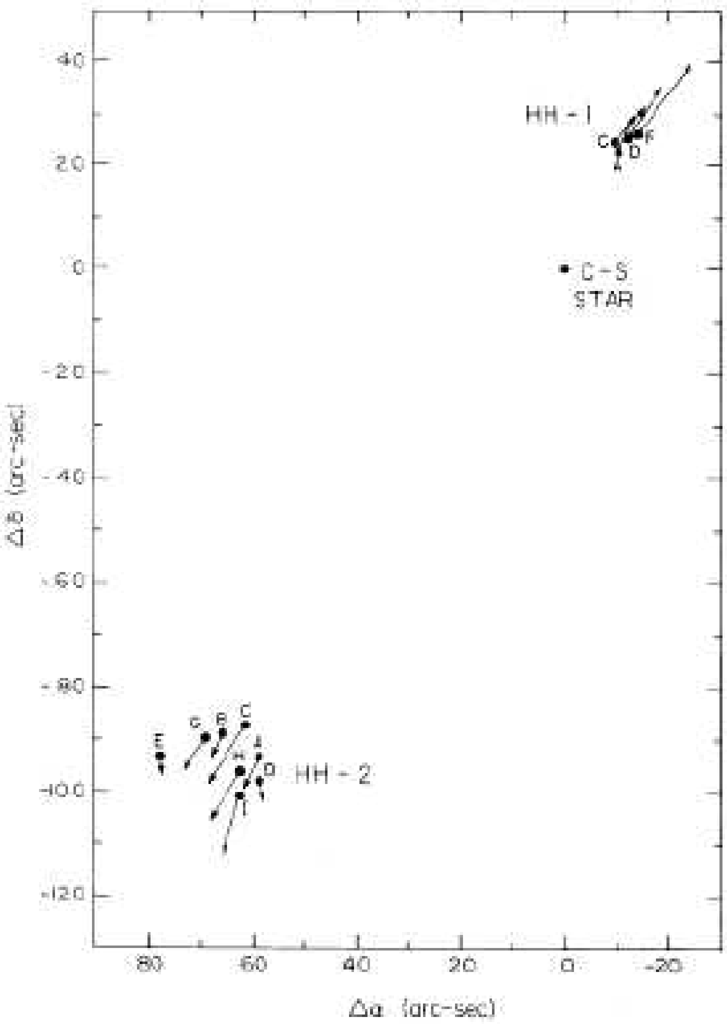

FIG. 7. The positions of HH 1, HH 2, and the Cohen-Schwartz star on the plane of the sky (for epoch 1968.0). The arrows indicate the shift in 100 yr due to proper motion. At a distance of 460 pc, 10 arcsec is equivalent to 2.23×10^{-2} pc. For HH 2A, the position is for A' although the motion vector is for A. The motion of the C-S star is too small to show on this scale. The internal motions in HH 1 and HH 2 are displayed at larger scale in Figs. 8 and 9.


HH 1
HH 2

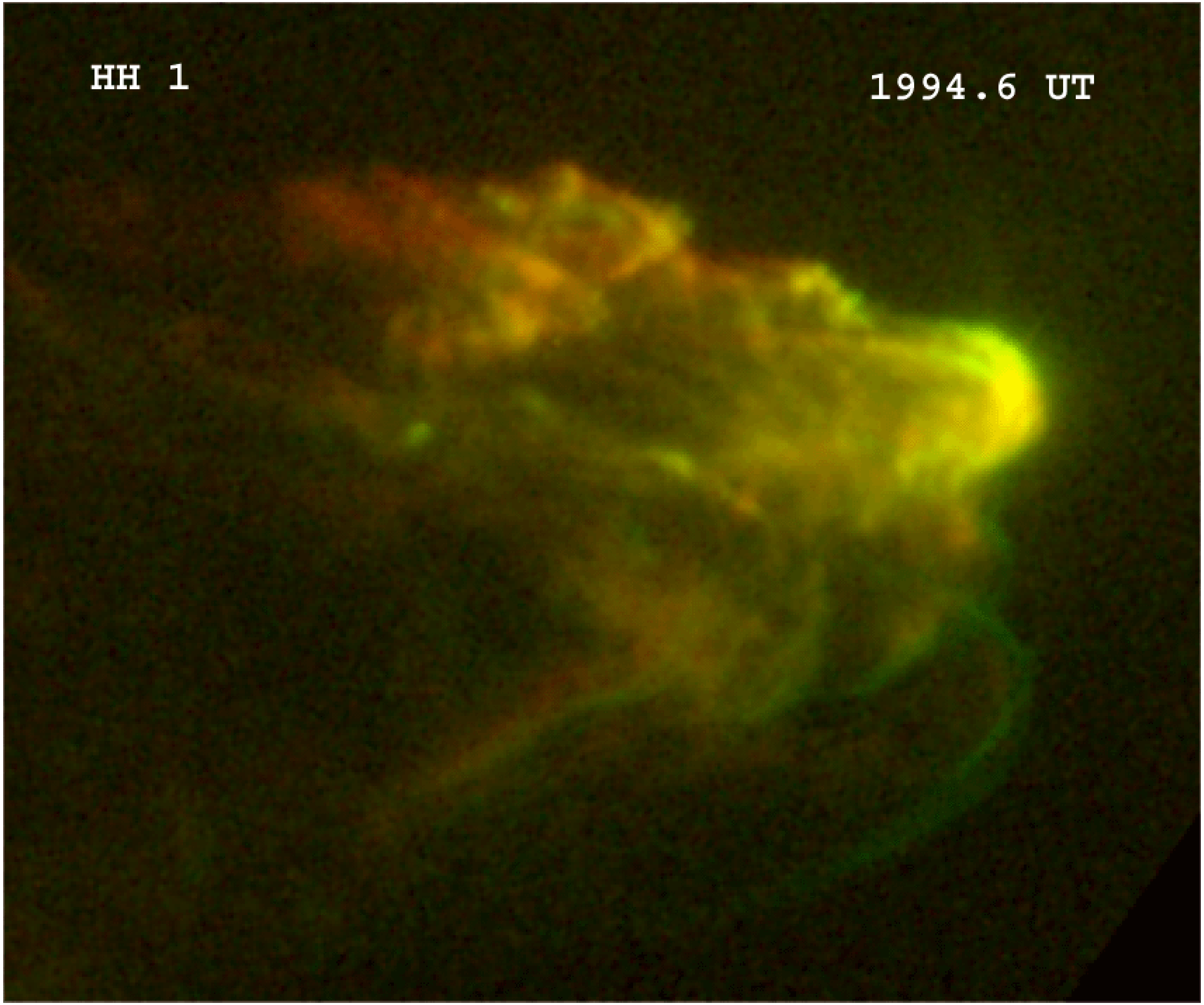
HH 1
1994.6 UT


Very Large Array

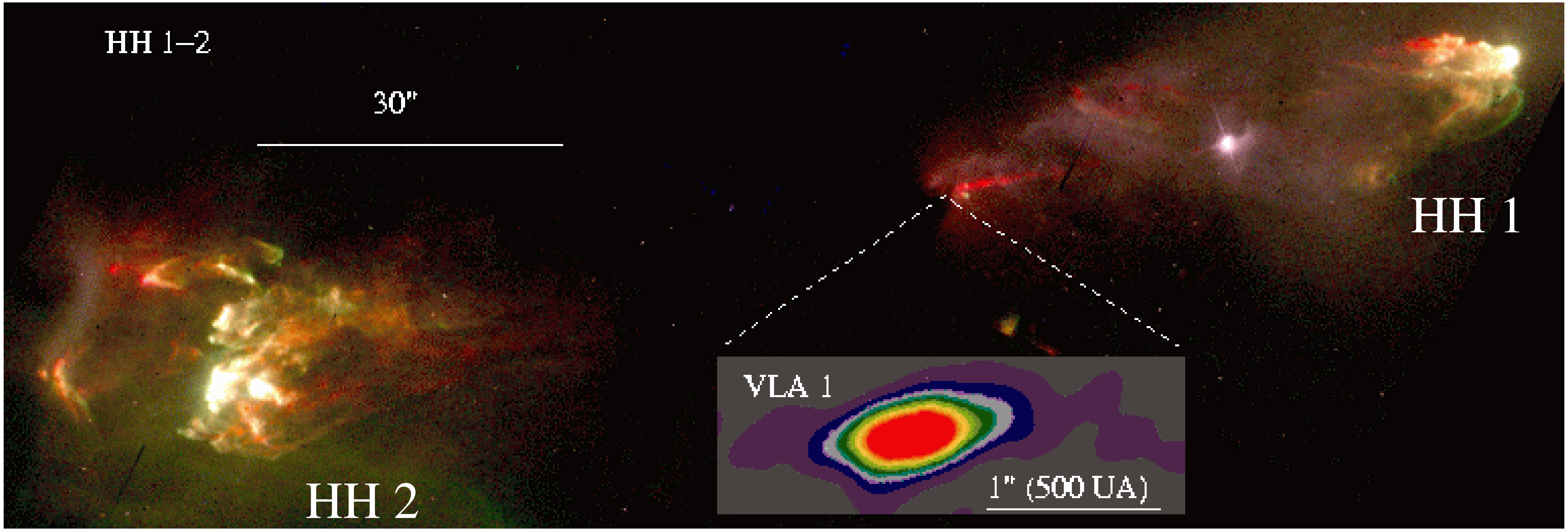
HH 1–2
30"
HH 1
HH 2
VLA 1
1" (500 UA)

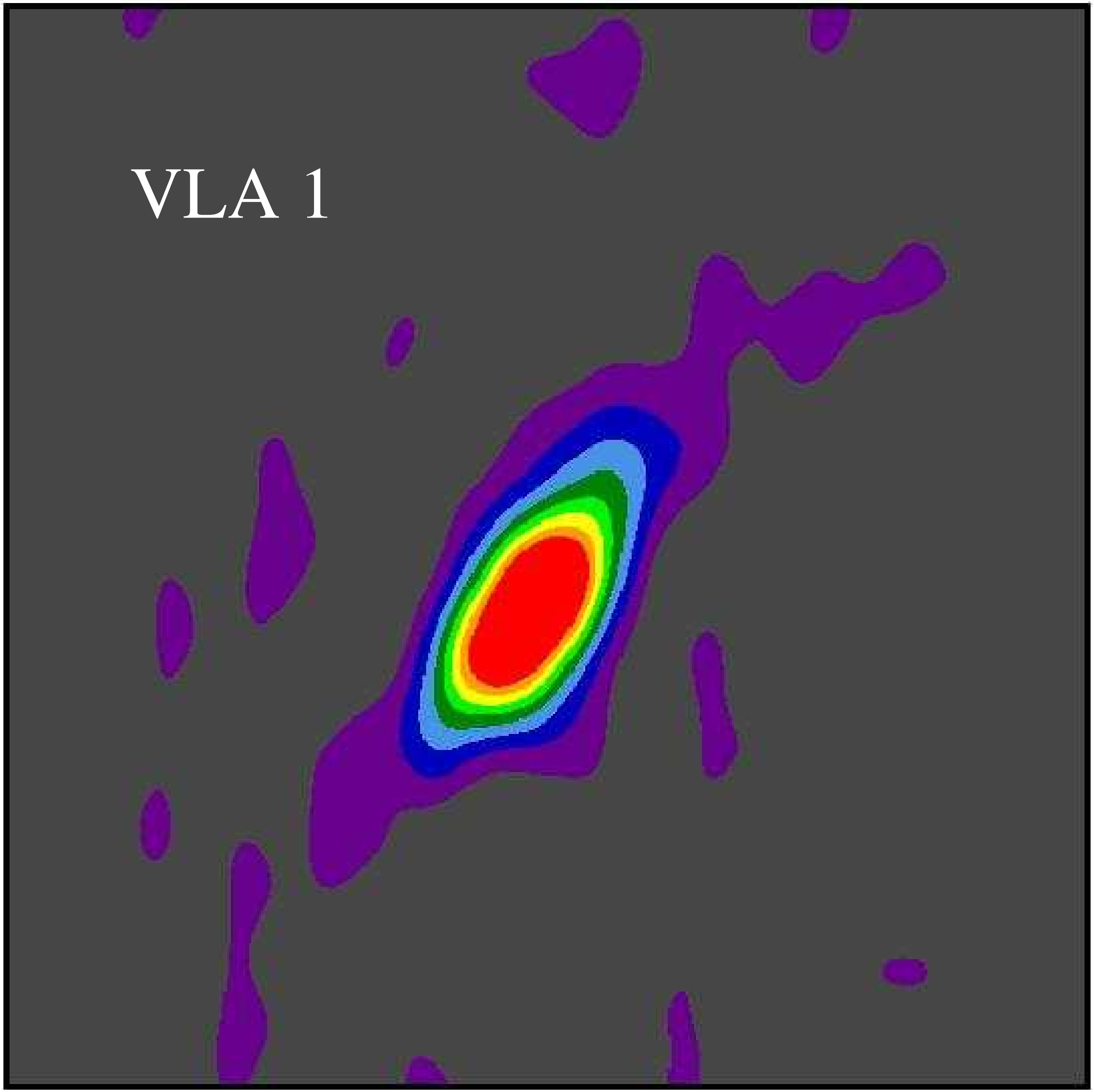
VLA 1

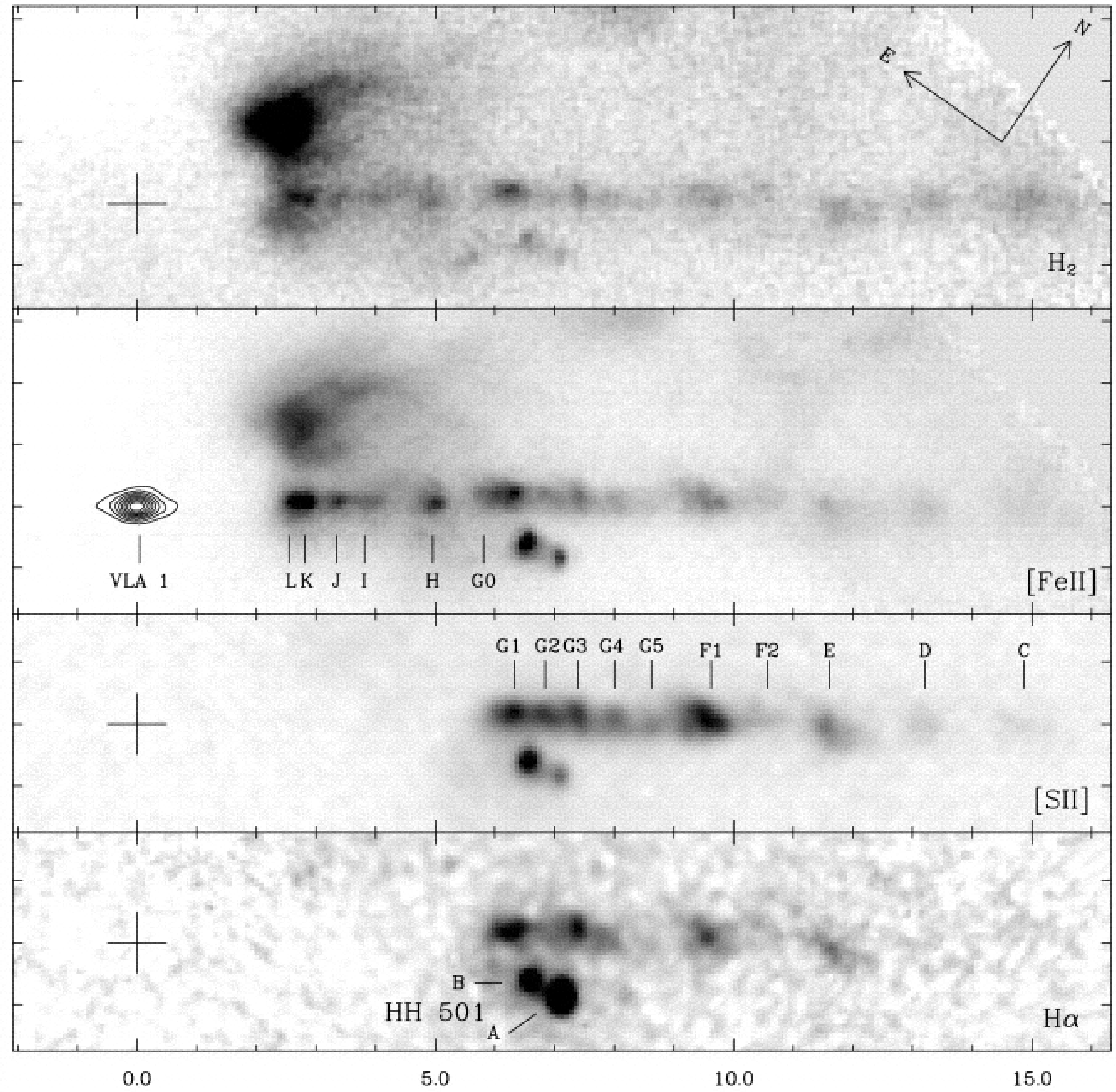

Complementarity of observations at different bands.

Reipurth et al. (2000) HST + VLA

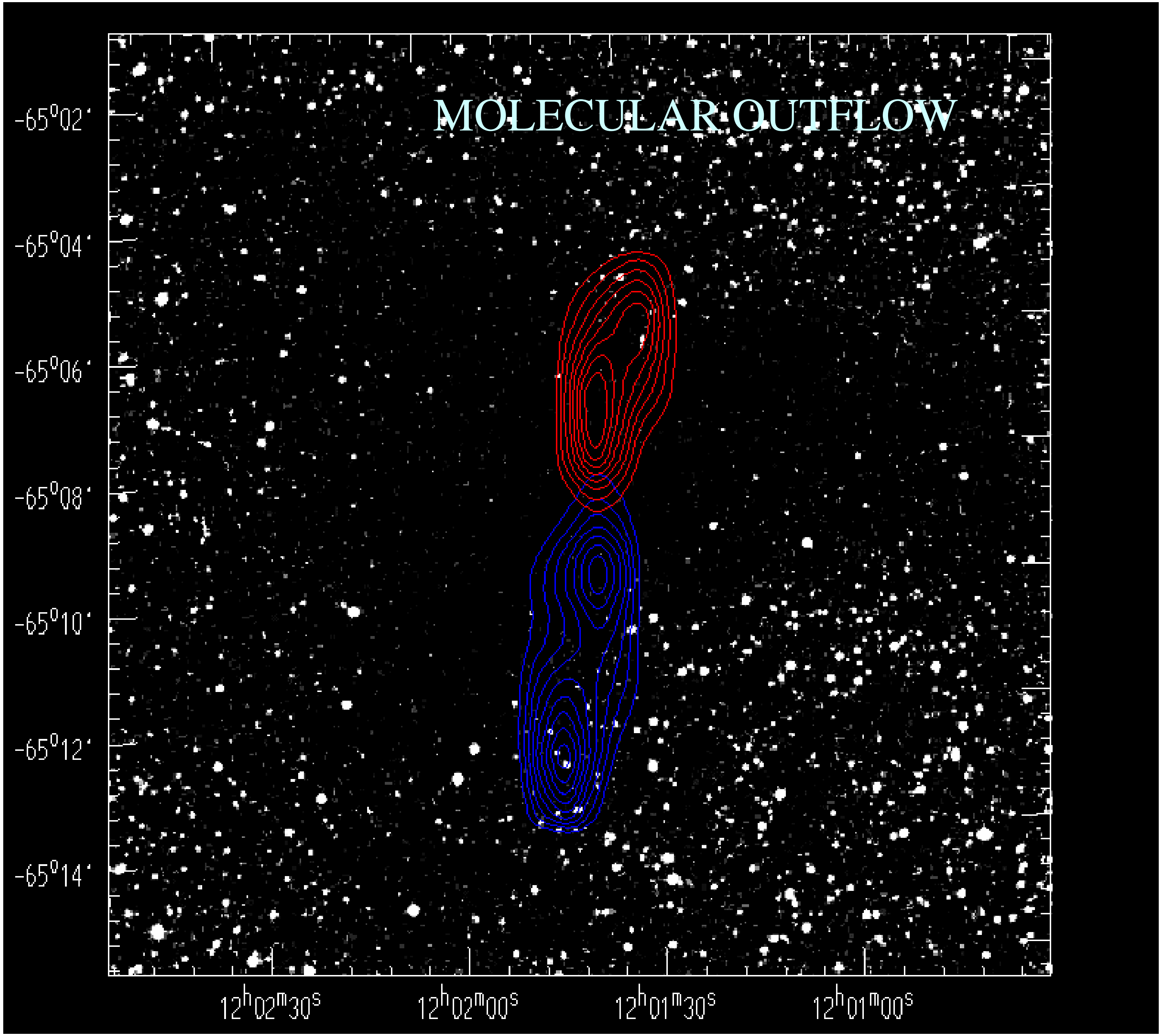

MOLECULAR OUTFLOW
-65°02'
-65°04'
-65°06'
-65°08'
-65°10'
-65°12'
-65°14'
12h02m30s
12h02m00s
12h01m30s
12h01m00s

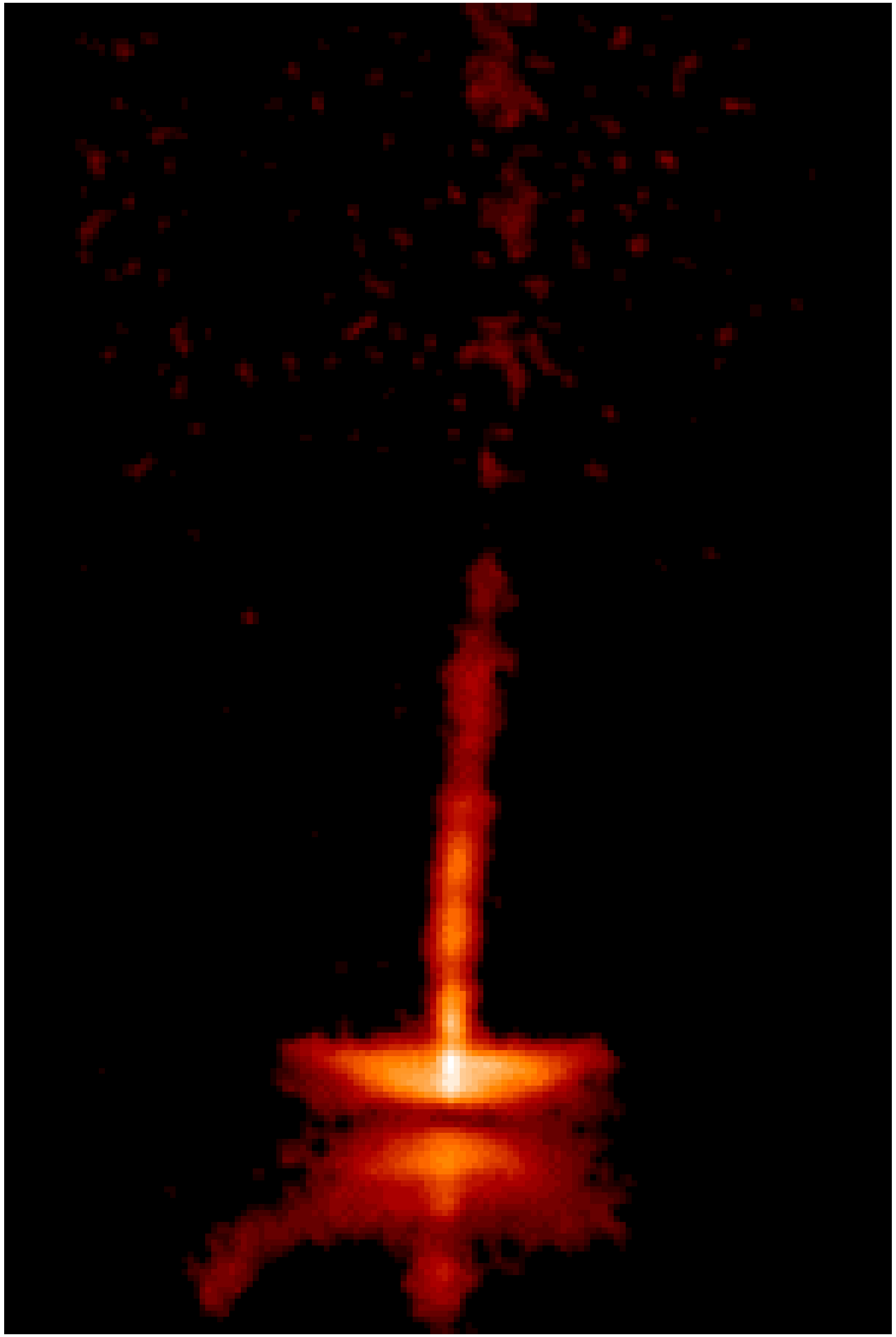

R-band HST images by Watson et al. of HH 30

<1980

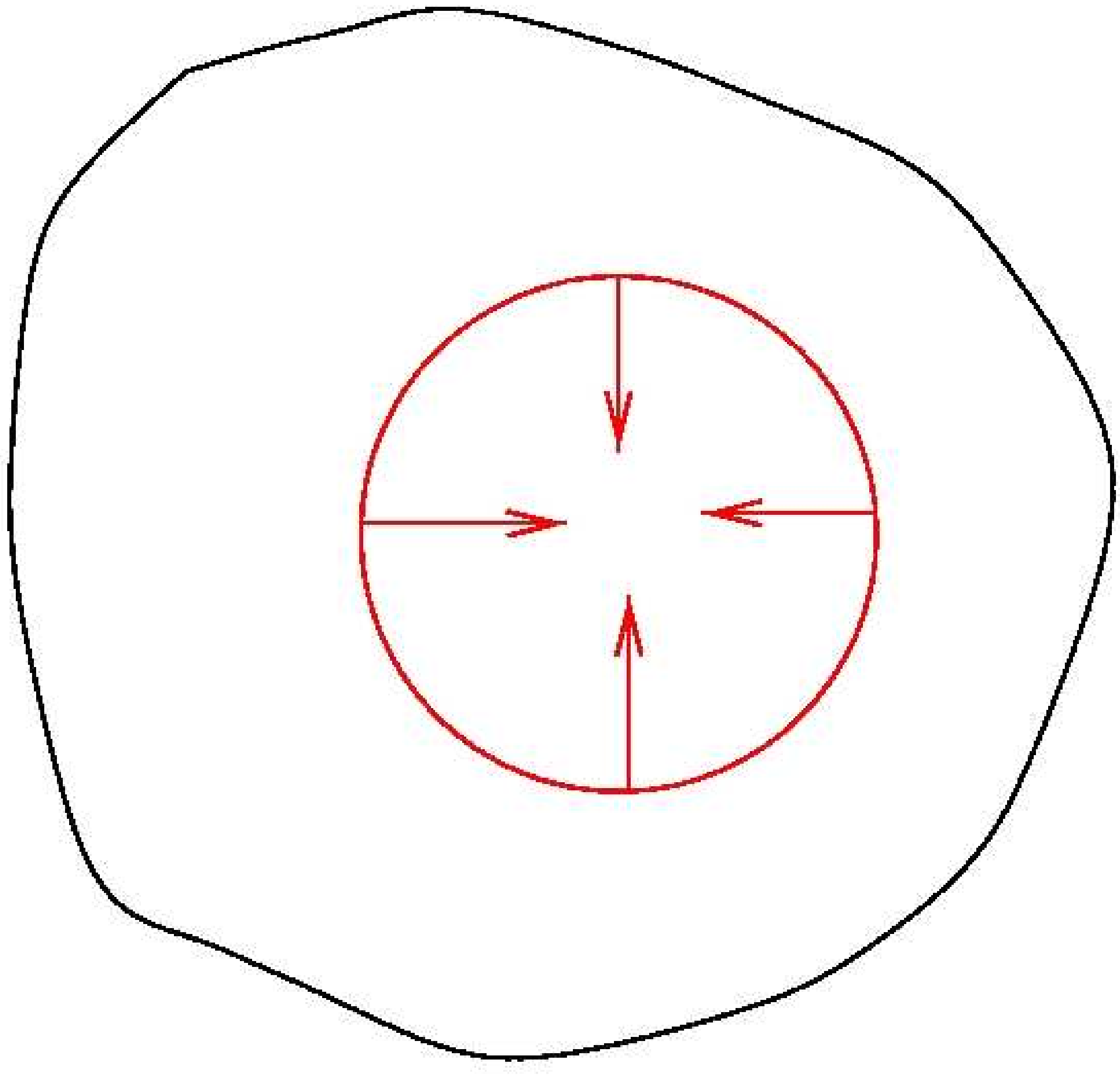

Current picture of low-mass star formation

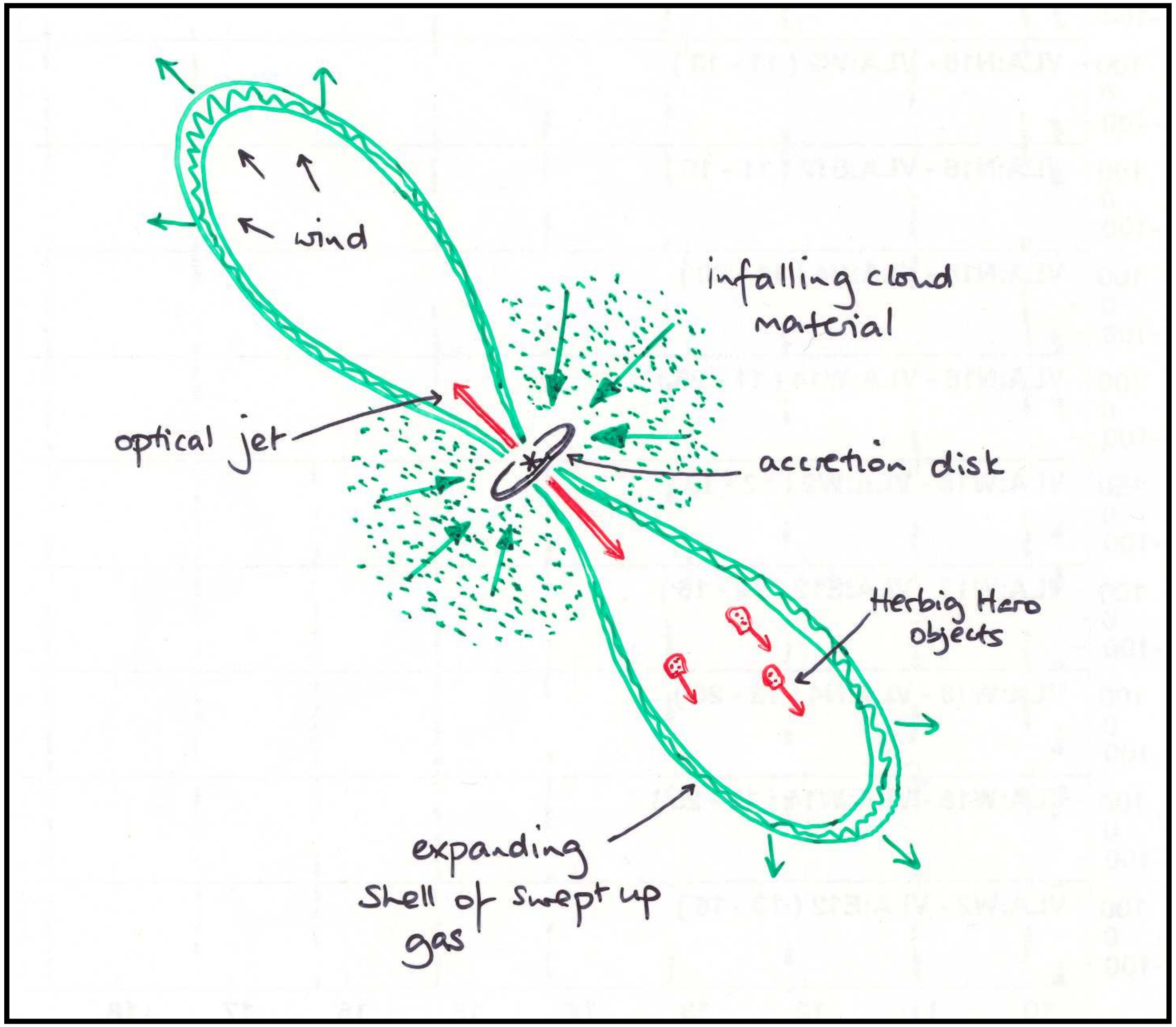

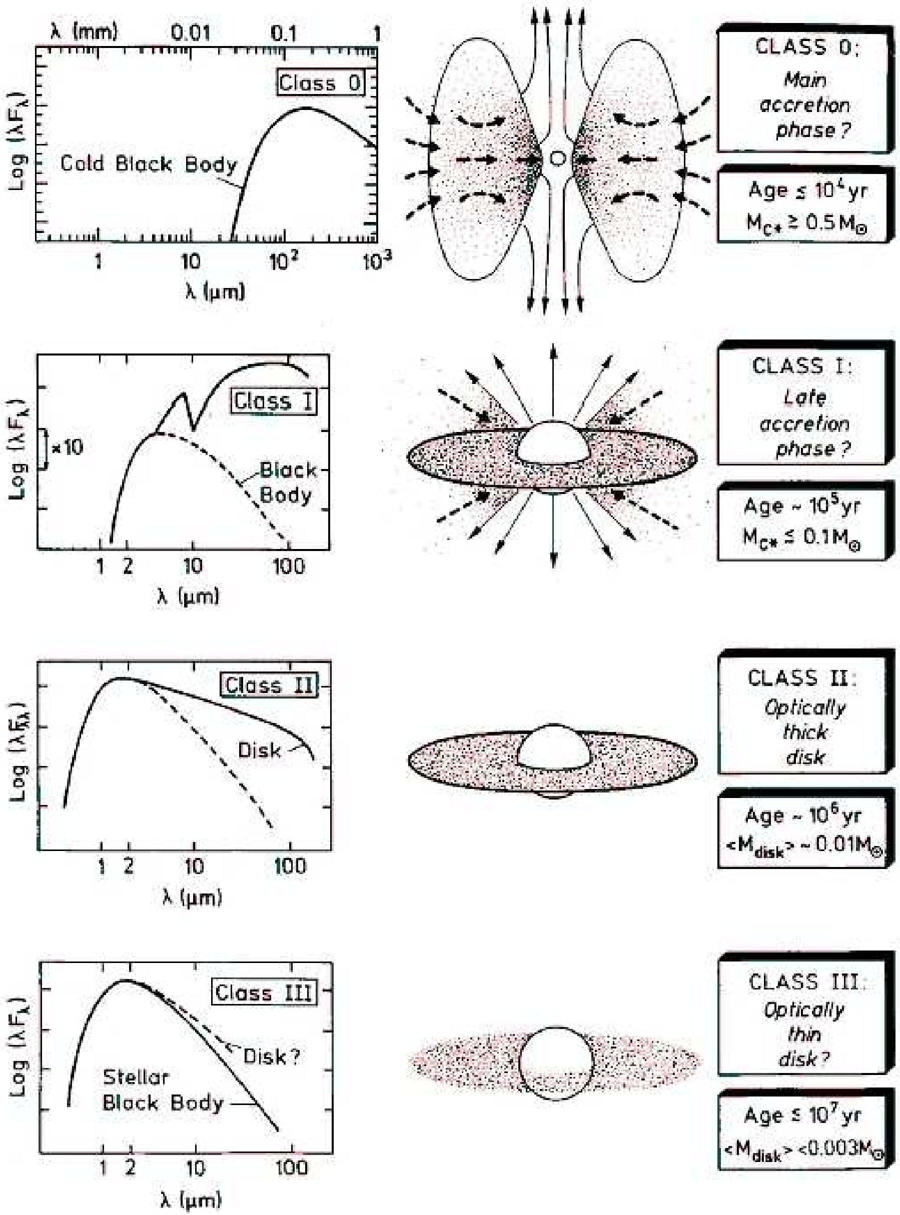

Figure 11 Evolutionary sequence of the spectral energy distributions for low-mass YSOs as proposed by André (1994). The four classes 0, I, II, and III correspond to successive stages of evolution.

Disk-Jet Symbiosis

- Disk: Forming star grows by accreting from disk (that accretes from envelope). Eventually, disk will condense into planets, asteroids, comets, etc.
- Jet: Carries away angular momentum and energy from disk, allowing accretion to proceed. They produce HH objects and molecular outflows, affecting energy balance and chemistry of cloud.

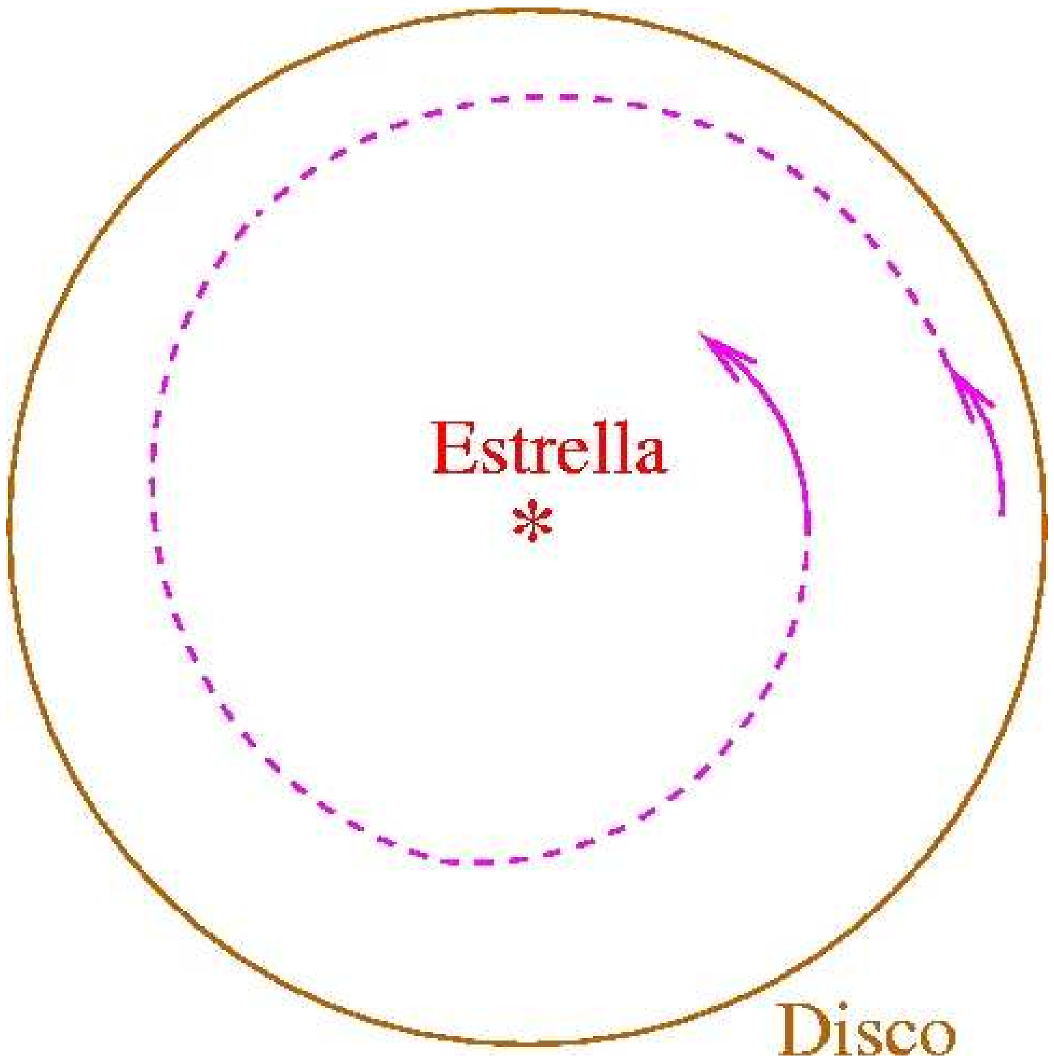

Gas “spirals” toward star

Total Energy Proportional to

$$-R^{-1}$$

Angular Momentum Proportional to

$$R^{1/2}$$

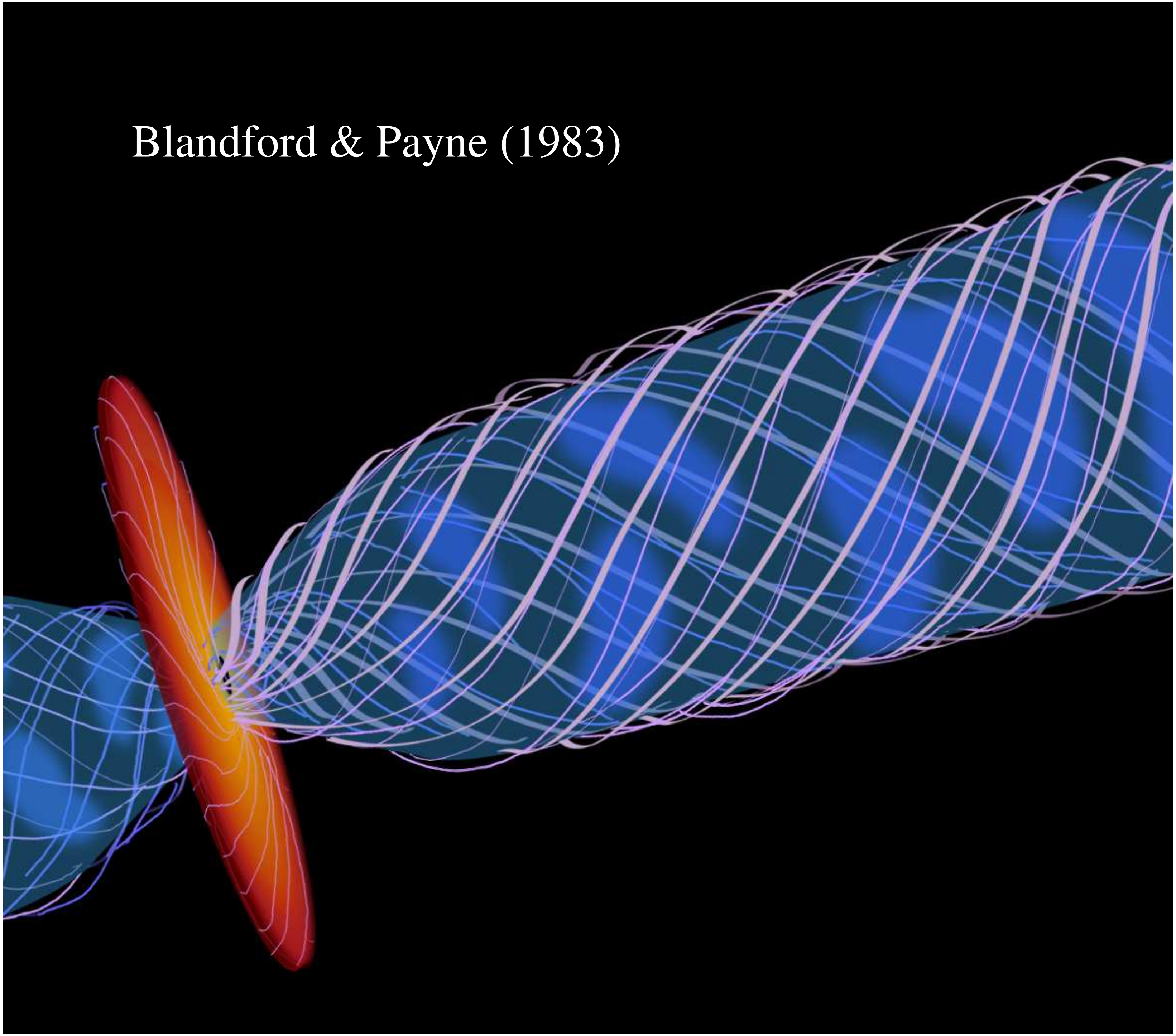
Blandford & Payne (1983)

Let´s take a look at the jets

- Free-free emission in the radio
- Base of jet usually heavily obscured
- Compact (<1”)

HII Regions

$$\Delta I_\nu = I_\nu(\tau_\nu) - I_\nu(0) = (F_\nu - I_\nu(0))(1 - e^{-\tau_\nu})$$

$I_\nu(0)$ is blackbody function at T_{bg} = 2.7 K (the cosmic microwave background).

F_ν is blackbody function at $T_{ex} \approx$ 10,000 K (the electron temperature of the ionized gas).

Neglect $I_\nu(0)$ to get

$$\Delta I_\nu = F_\nu \, (1 - e^{-\tau_\nu})$$

Since $S_\nu = \Delta I_\nu \Omega_\nu$, and using R-J approximation:

$$S_\nu = \frac{2kT_e\nu^2}{c^2}(1 - e^{-\tau_\nu})\,\Omega_\nu$$

HII Regions

$$S_\nu = \frac{2kT_e\nu^2}{c^2}(1-e^{-\tau_\nu})\,\Omega_\nu$$

$$\tau_\nu \propto n_e^2\, l\, \nu^{-2.1}$$

For (more or less) homogeneous HII region, Ω_ν is approximately constant with ν. We then have the two limit cases for $\tau_\nu > 1$ (low frequencies) and for $\tau_\nu < 1$ (high frequencies):

$S_\nu \propto \nu^2$ (optically thick)

$S_\nu \propto \nu^{-0.1}$ (optically thin)

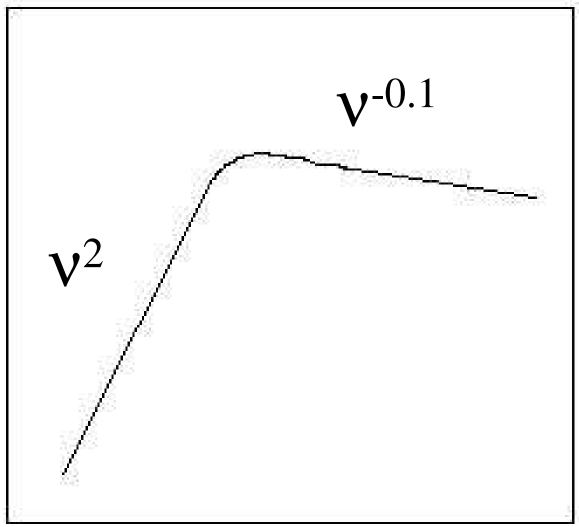

Thermal Jets

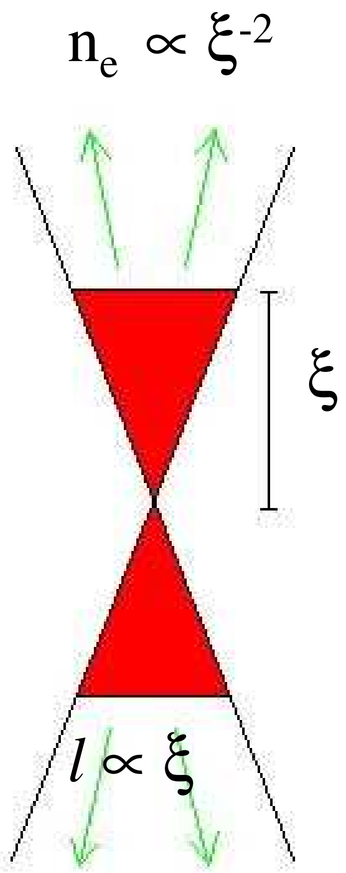

$$\tau_\nu(\xi) \propto n_e^2 \, l \, \nu^{-2.1}$$

$$\tau_\nu(\xi) \propto \xi^{-3} \nu^{-2.1}$$

We define ξ_c when $\tau_\nu(\xi_c) = 1$

Then $\xi_c \propto \nu^{-0.7}$ => size of source decreases with ν!

Since $S_\nu \propto \nu^2 \, \xi^2_c \propto \nu^2 \, \nu^{-1.4} \propto \nu^{0.6}$

$\theta_\nu \propto \nu^{-0.7}$ $\qquad\qquad$ $S_\nu \propto \nu^{0.6}$

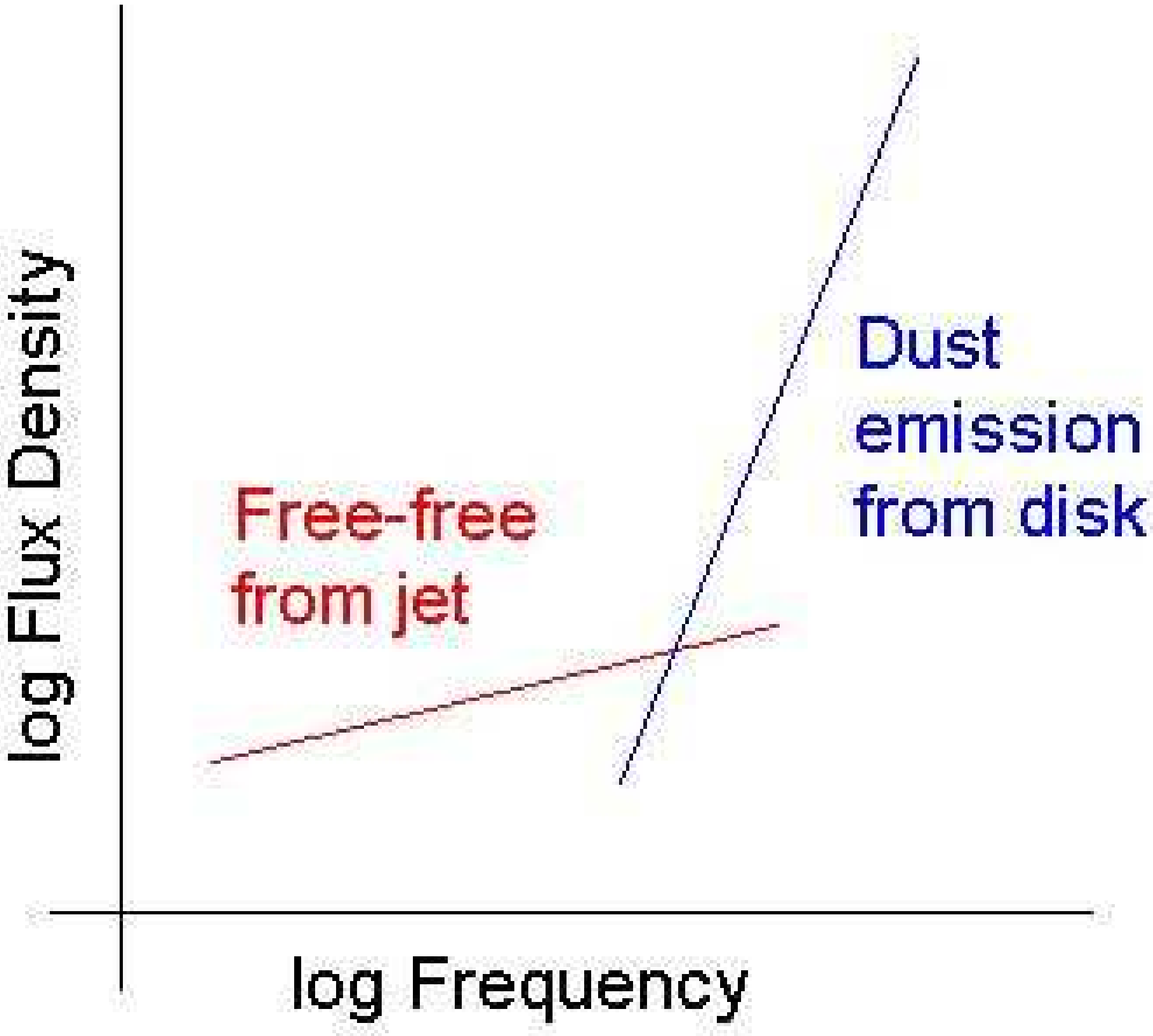

Free-free emission from ionized gas in jet dominates cm region, while thermal emission from dust in the disk dominates mm region.

Dust Emission

$$\Delta I_\nu = I_\nu(\tau_\nu) - I_\nu(0) = (F_\nu - I_\nu(0))(1 - e^{-\tau_\nu})$$

$I_\nu(0)$ is blackbody function at T_{bg} = 2.7 K (the cosmic microwave background).

F_ν is blackbody function at $T_d \approx$ 10-300 K (the temperature of the dust).

Neglect $I_\nu(0)$ to get

$$\Delta I_\nu = F_\nu \,(1 - e^{-\tau_\nu})$$

Since $S_\nu = \Delta I_\nu \Omega_\nu$, and using R-J approximation:

$$S_\nu = \frac{2kT_d \nu^2}{c^2}(1 - e^{-\tau_\nu})\,\Omega_\nu$$

Dust Emission

$$S_\nu = \frac{2kT_d\nu^2}{c^2}(1-e^{-\tau_\nu})\Omega_\nu$$

$$\tau_\nu \propto n_d\, l\, \nu^{0-2}$$

For (more or less) homogeneous dust region, Ω_ν is approximately constant with ν. We then have the two limit cases for $\tau_\nu > 1$ (low frequencies) and for $\tau_\nu < 1$ (high frequencies):

$S_\nu \propto \nu^2$ (optically thick at high ν, IR wavelengths)

$S_\nu \propto \nu^{2\text{-}4}$ (optically thin at low ν, millimeter wavelenghts)

Power law index of opacity depends, to first approximation, on relative sizes between grain of dust and wavelength of radiation:
$a \ll \lambda \rightarrow 2$; $a \gg \lambda \rightarrow 0$

Dust Emission

If dust is optically thin:

$$S_\nu \propto T_d \; n_d \, l \, \Omega \; \nu^{\,2-4}$$; and since

$$n_d \, l \, \Omega = n_d \frac{V}{d^2} = \frac{M_d}{d^2}$$

$$S_\nu \propto T_d \frac{M_d}{d^2} \nu^{\,2-4}$$

If you know flux density, dust temperature, distance to source, and opacity characteristics of dust, you can get M_d.

Assume dust to gas ratio and you get total mass of object.

Three (multiple) young, low-mass systems

- L1551 IRS5
- HH 111
- HH 7-11
- Tomorrow: Massive star formation

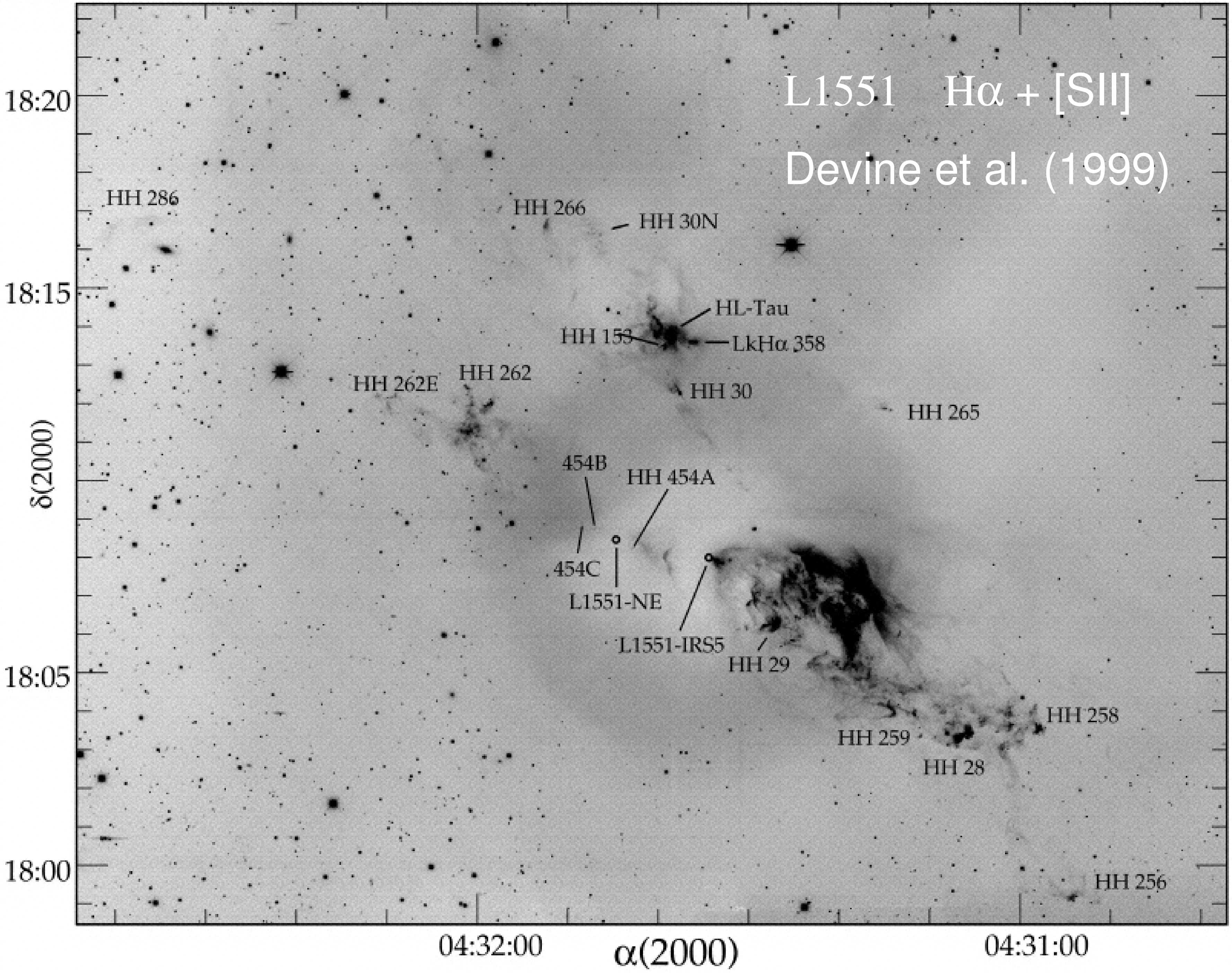

L1551 Hα + [SII]
Devine et al. (1999)
HH 286
HH 266
HH 30N
HL-Tau
HH 153
LkHα 358
HH 262E
HH 262
HH 30
HH 265
454B
HH 454A
454C
L1551-NE
L1551-IRS5
HH 29
HH 259
HH 28
HH 258
HH 256
18:20
18:15
18:05
18:00
δ(2000)
04:32:00
04:31:00
α(2000)

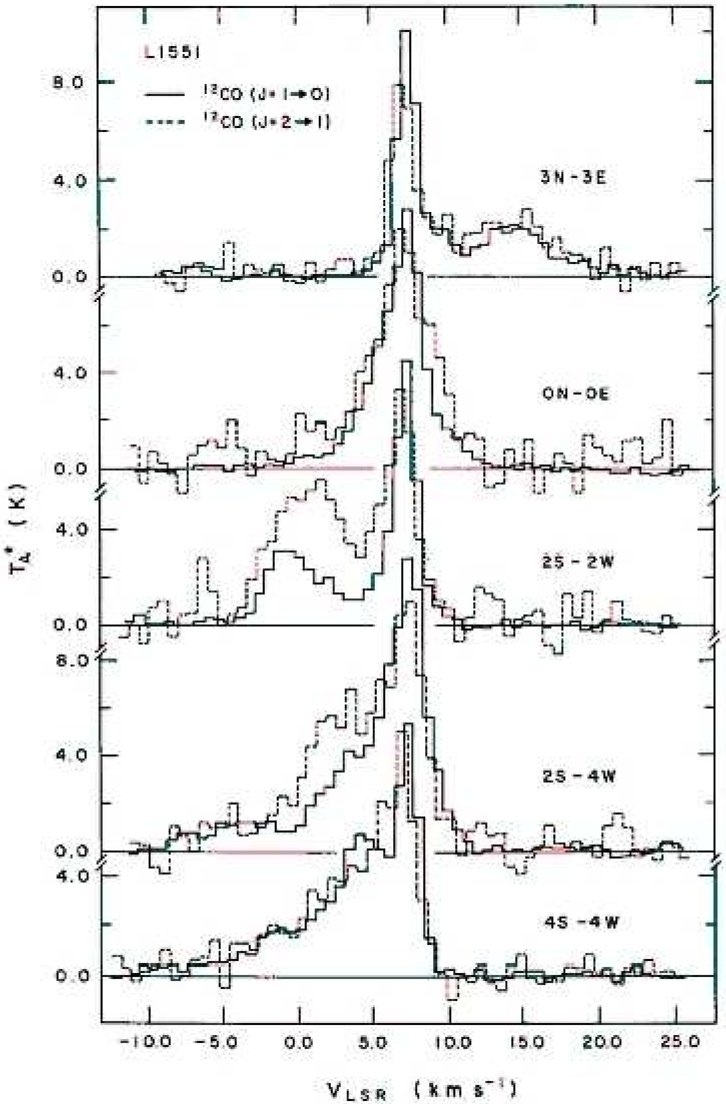

FIG. 1.—Spectra of the J = 1–0 (*solid*) and J = 2–1 (*dashed*) lines of ^{12}CO taken toward five selected positions in L1551. Offsets are measured in arcmin relative to the position of IRS-5 at α(1950) = 04^{h}28^{m}40^s, δ(1950) = 18°01′52″. The J = 1–0 spectra were taken at NRAO with a 1′.1 beam; the J = 2–1 spectra were taken at the MWO with a 1′.2 beam. The ratio of the 2–1 and 1–0 antenna temperatures in the broad velocity features can be used to infer the kinetic temperature of the gas responsible for these features.

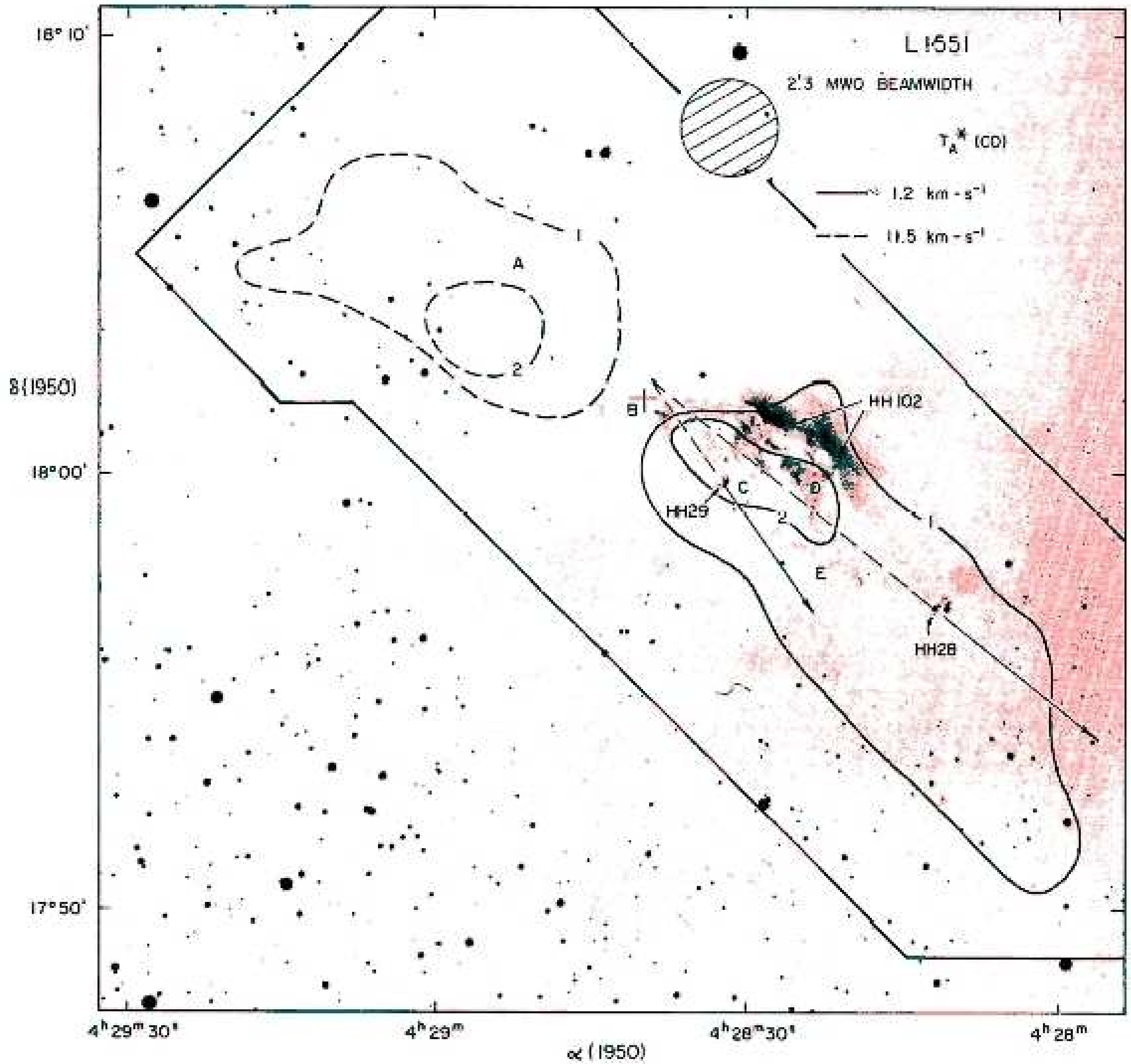

FIG. 2.—Contour map of the $J = 1$–0 ^{12}CO antenna temperatures in the broad velocity components, superposed on an optical photo of the region taken by Strom with the 4 m telescope at KPNO. The map is based on CO spectra taken at 115 positions within the enclosed border with 1′–2′ spacings. A cross indicates the position of IRS-5; letters A–E indicate the positions of the five spectra in Fig. 1 from top to bottom. Also shown are the directions of the proper motions of the two compact Herbig-Haro objects, HH28 and HH29; tracing their motion backward suggests a common origin at the infrared source.

L1551 IRS5

- Near-IR source (Strom et al. 1976) that excites bipolar outflow (Snell et al. 1980)
- Located in Taurus at 140 pc
- Bolometric luminosity of 30 L_{SUN}
- Embedded in dense core (1000 AU)
- Believed to be prototype of single star in formation

BIMA

Looney et al. 1997 2.7 mm

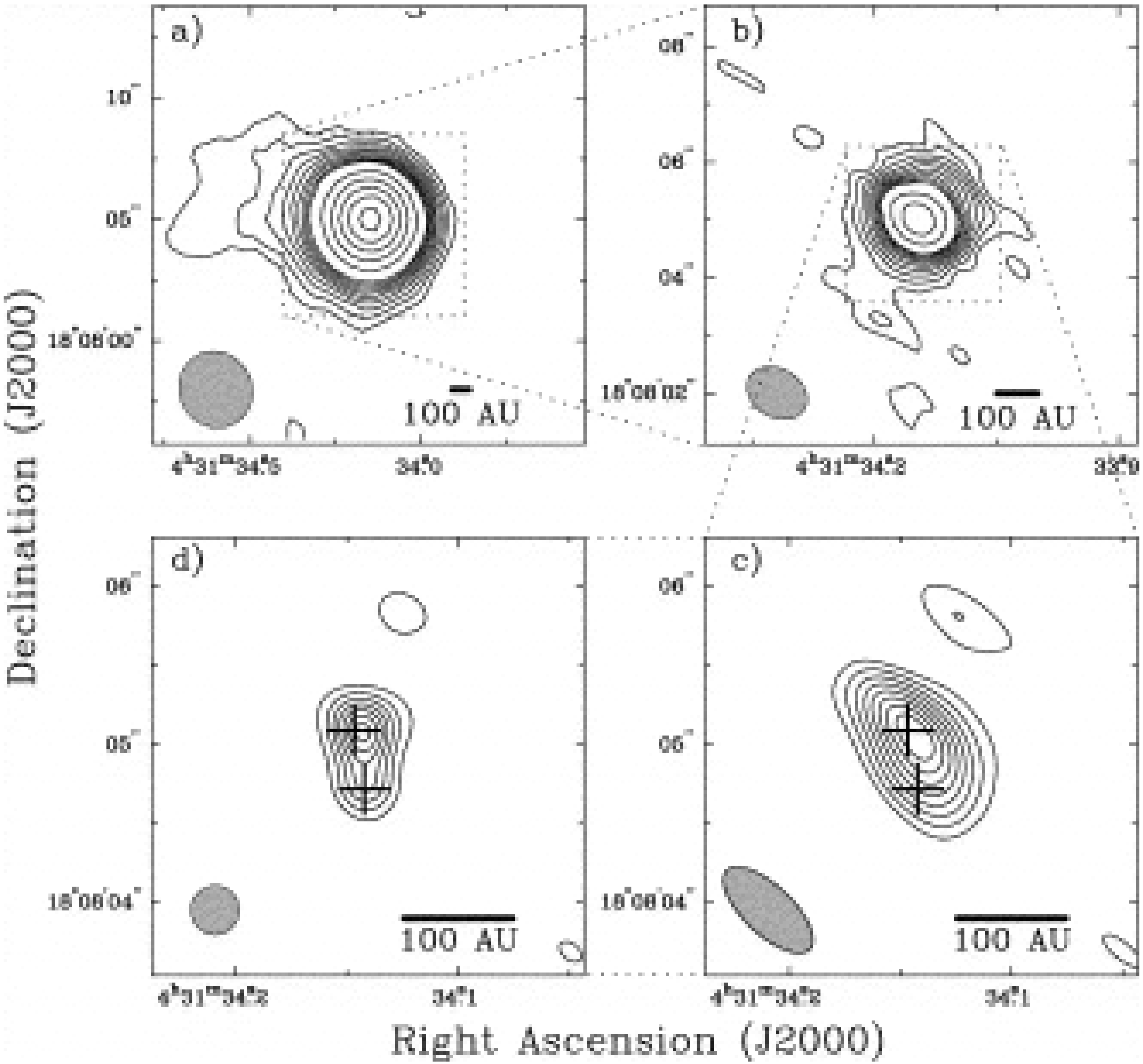


Very Large Array

Rodríguez et al. 1998

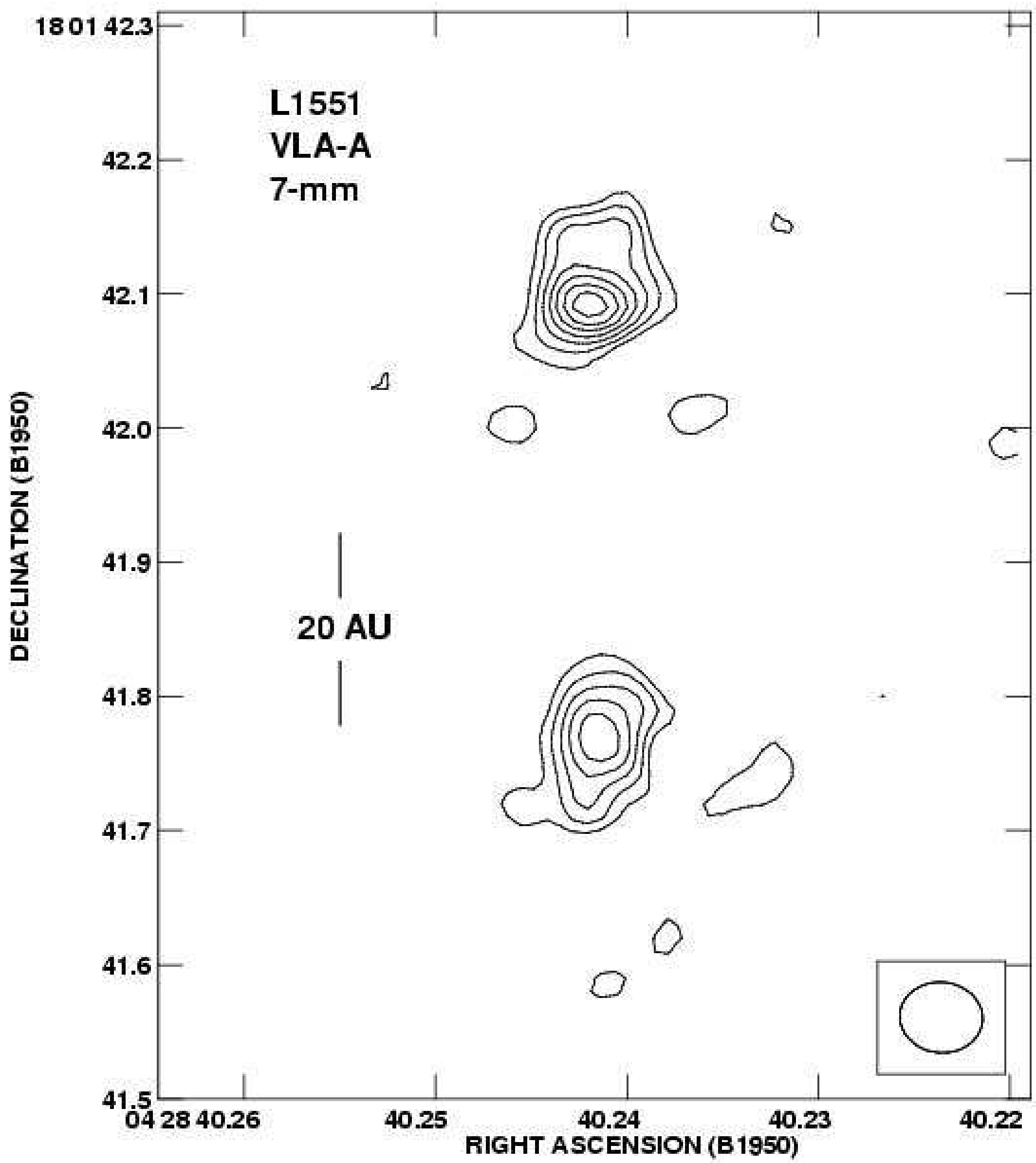

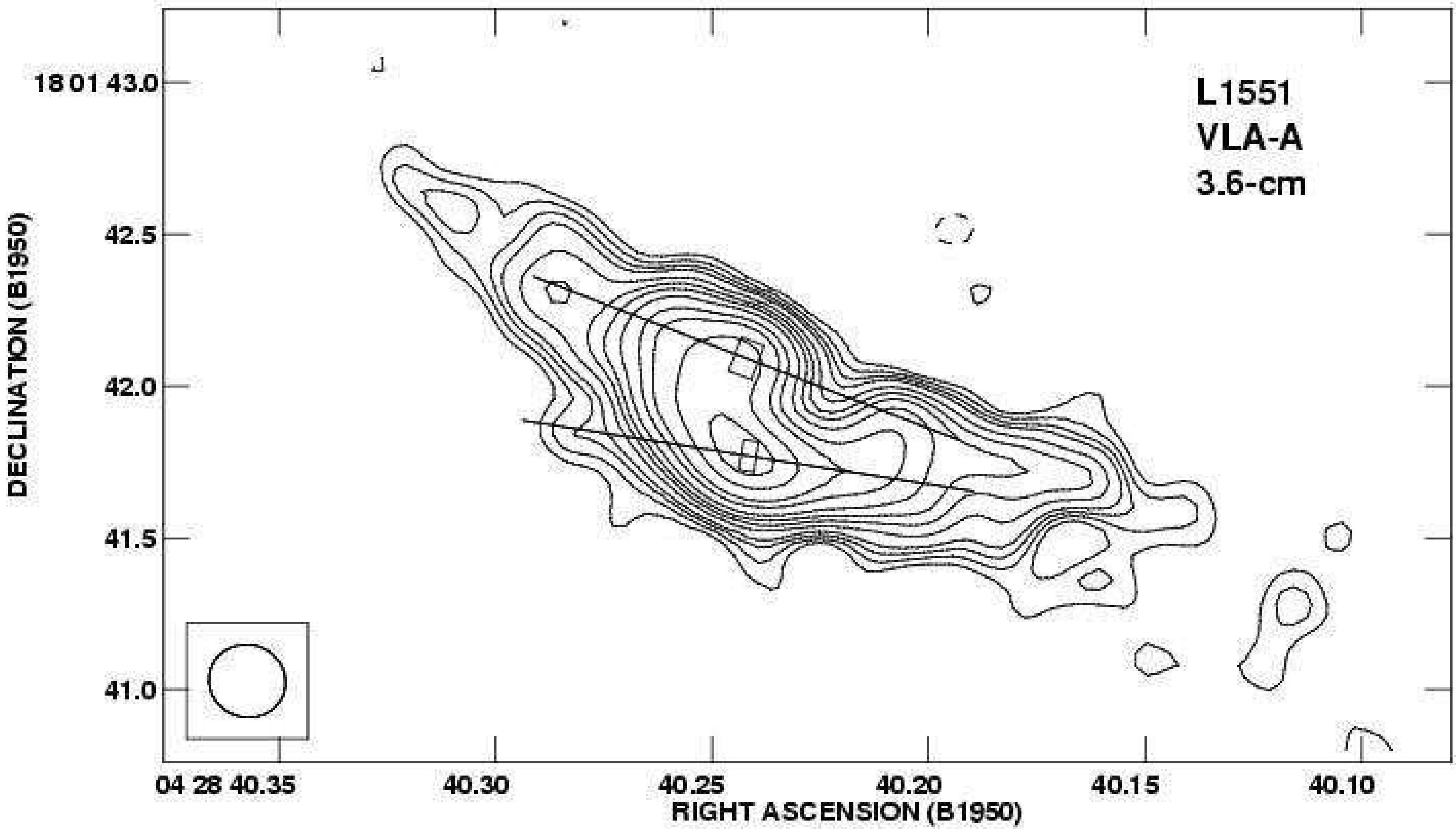
L1551
VLA-A
3.6-cm
DECLINATION (B1950)
18 01 43.0
42.5
42.0
41.5
41.0
04 28 40.35
40.30
40.25
40.20
40.15
40.10
RIGHT ASCENSION (B1950)

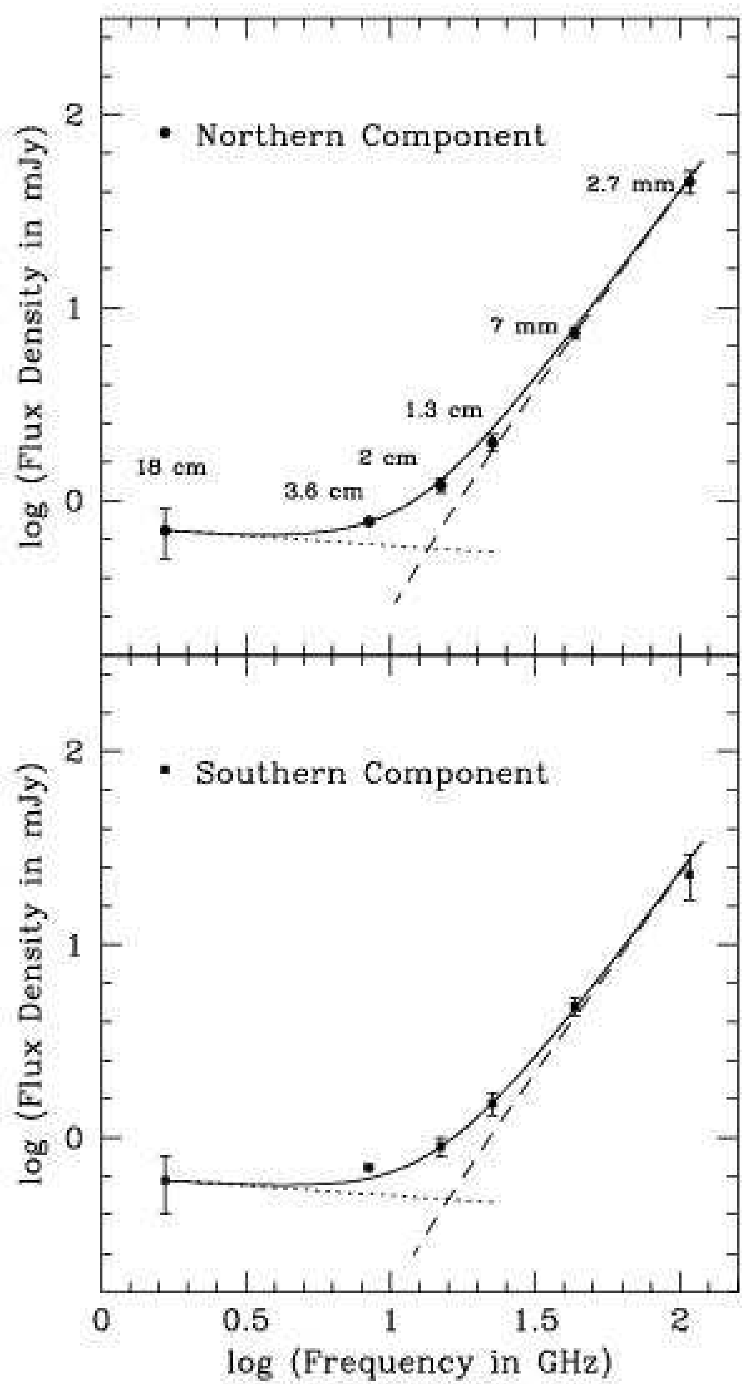

Free-free from ionized outflow dominates cm range, while thermal emission from dust in disk dominates mm range

L1551 IRS5

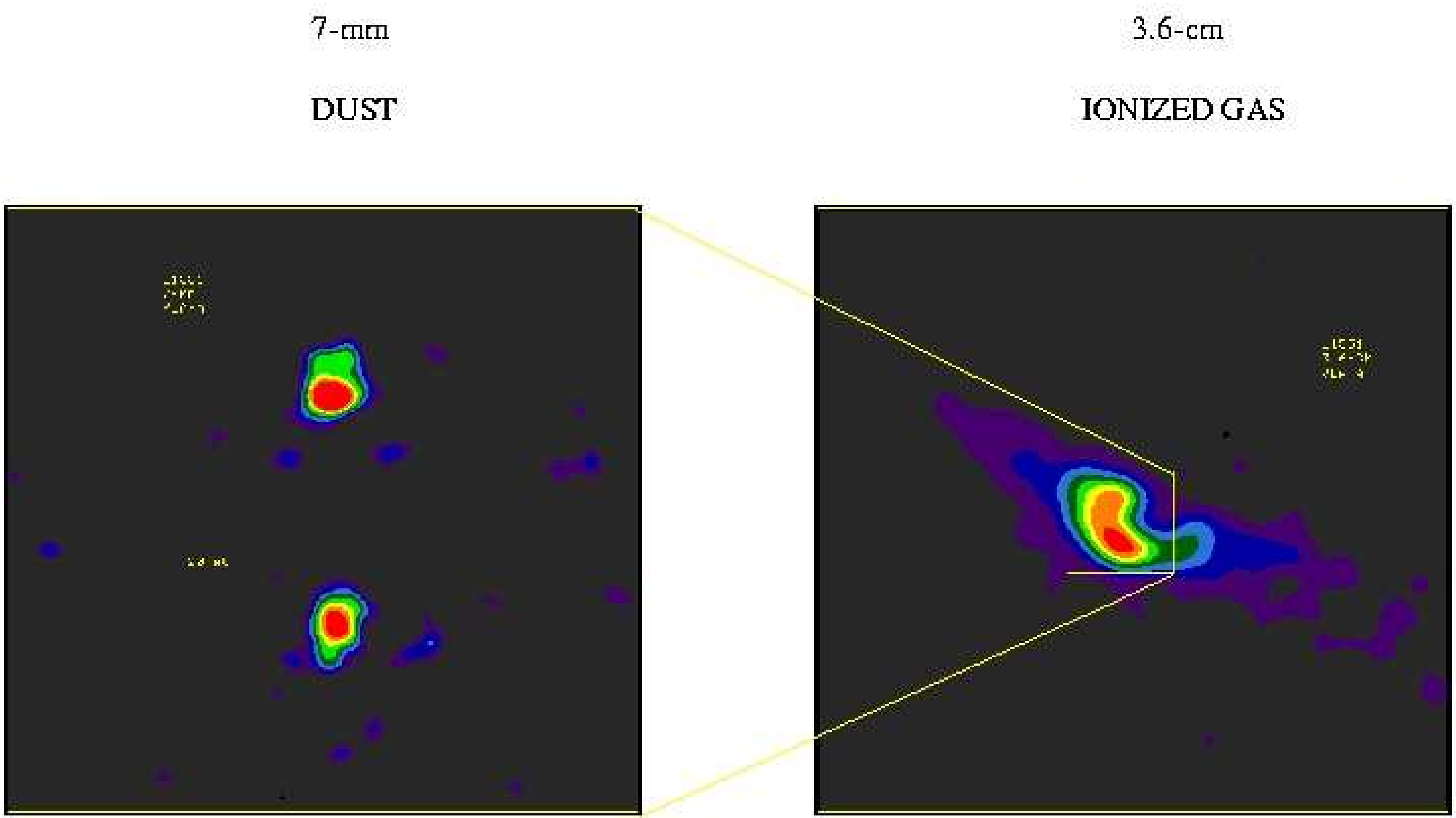

As the angular resolution of an interferometer is

$\theta = \lambda / B$

You cannot compare observations at 3.6 cm and 7 mm made with the same baseline B.

Two stars...

Two disks...

Two jets?

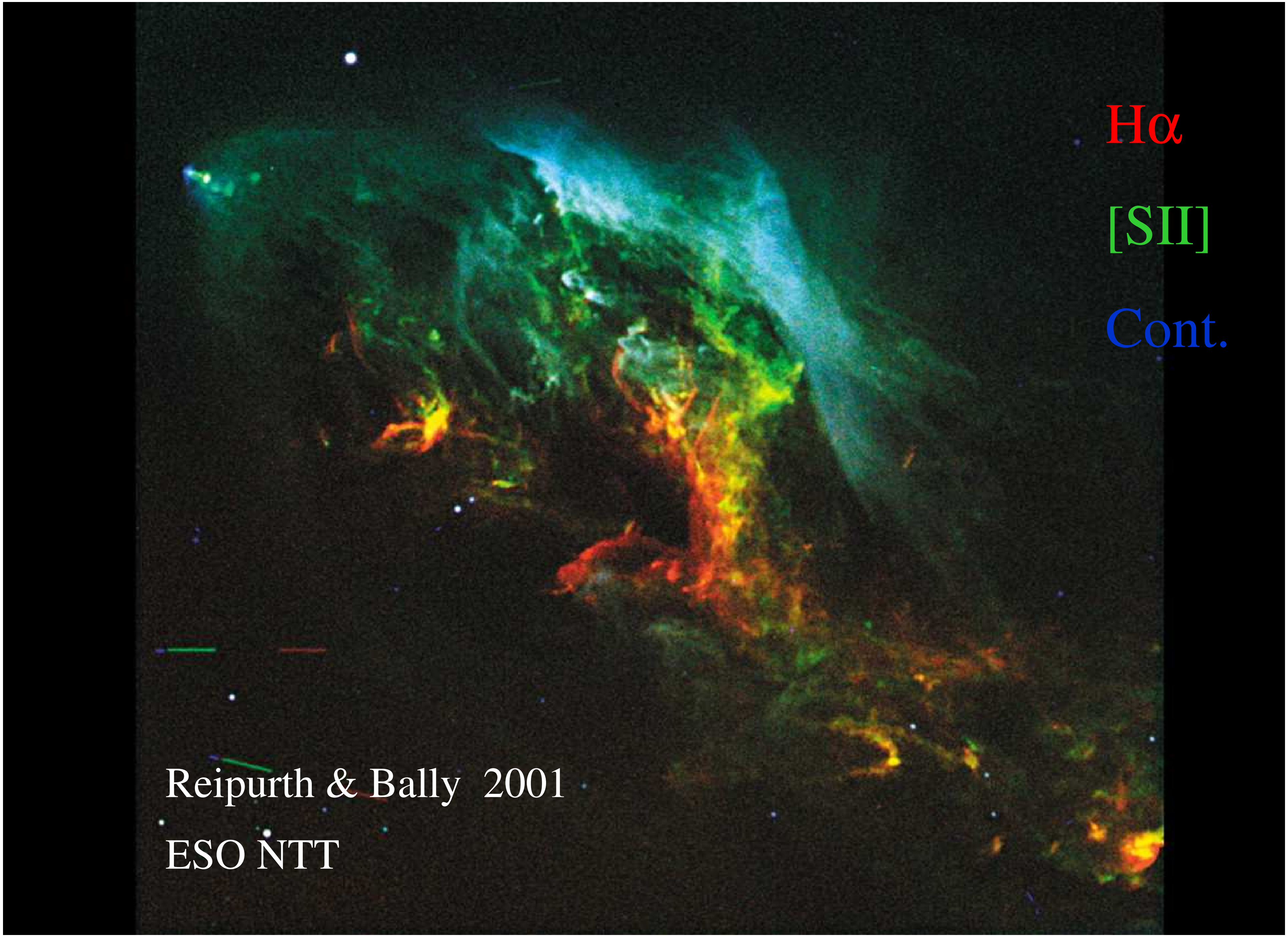
Hα
[SII]
Cont.
Reipurth & Bally 2001
ESO NTT

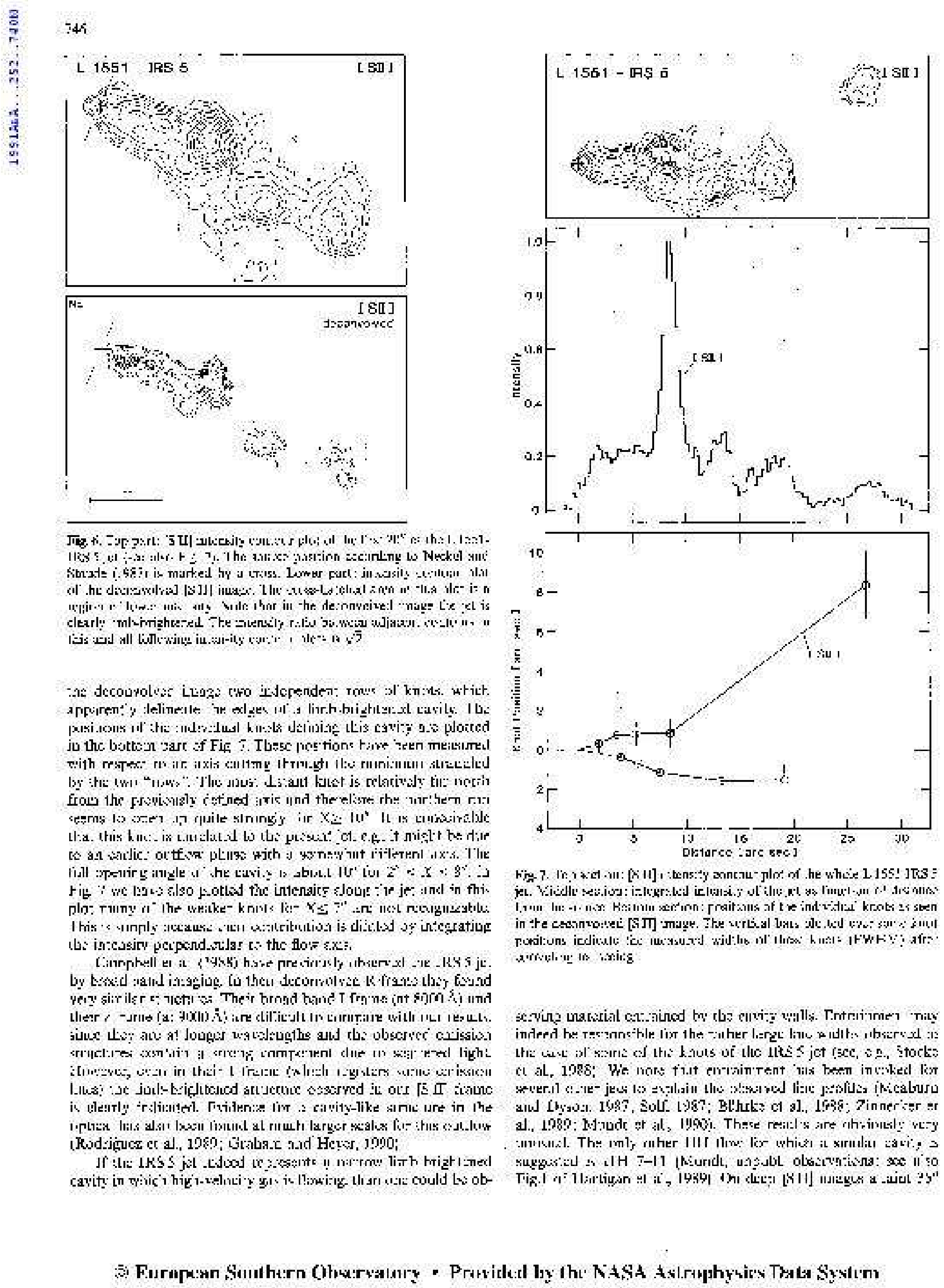

Fig. 6. Top part: [S II] intensity contour plot of the first 20" of the L 1551-IRS 5 jet (see also Fig. 7). The source position according to Neckel and Staude (1987) is marked by a cross. Lower part: intensity contour plot of the deconvolved [S II] image. The cross-hatched area of this plot is a region of lower intensity. Note that in the deconvolved image the jet is clearly limb-brightened. The intensity ratio between adjacent contours in this and all following intensity contour plots is √2

the deconvolved image two independent rows of knots, which apparently delineate the edges of a limb-brightened cavity. The positions of the individual knots defining this cavity are plotted in the bottom part of Fig. 7. These positions have been measured with respect to an axis cutting through the minimum straddled by the two "rows". The most distant knot is relatively far north from the previously defined axis and therefore the northern rim seems to open up quite strongly for X ≥ 10". It is conceivable that this knot is unrelated to the present jet, e.g. it might be due to an earlier outflow phase with a somewhat different axis. The full opening angle of the cavity is about 10° for 2" < X < 8". In Fig. 7 we have also plotted the intensity along the jet and in this plot many of the weaker knots for X ≤ 7" are not recognizable. This is simply because their contribution is diluted by integrating the intensity perpendicular to the flow axis.

Campbell et al. (1988) have previously observed the IRS 5 jet by broad band imaging. In their deconvolved R frame they found very similar structures. Their broad band I frame (at 8000 Å) and their z frame (at 9000 Å) are difficult to compare with our results, since they are at longer wavelengths and the observed emission structures contain a strong component due to scattered light. However, even in their I frame (which registers some emission lines) the limb-brightened structure observed in our [S II] frame is clearly indicated. Evidence for a cavity-like structure in the optical has also been found at much larger scales for this outflow (Rodríguez et al., 1989; Graham and Heyer, 1990).

If the IRS 5 jet indeed represents a narrow limb brightened cavity in which high-velocity gas is flowing, then one could be ob-

Fig. 7. Top section: [S II] intensity contour plot of the whole L 1551 IRS 5 jet. Middle section: integrated intensity of the jet as function of distance from the source. Bottom section: positions of the individual knots as seen in the deconvolved [S II] image. The vertical bars plotted over some knot positions indicate the measured widths of these knots (FWHM) after correcting for seeing.

serving material entrained by the cavity walls. Entrainment may indeed be responsible for the rather large line widths observed in the case of some of the knots of the IRS 5 jet (see, e.g., Stocke et al., 1988). We note that entrainment has been invoked for several other jets to explain the observed line profiles (Meaburn and Dyson, 1987; Solf, 1987; Bührke et al., 1988; Zinnecker et al., 1989; Mundt et al., 1990). These results are obviously very unusual. The only other HH flow for which a similar cavity is suggested is HH 7–11 (Mundt, unpubl. observations; see also Fig. 1 of Hartigan et al., 1989). On deep [S II] images a faint 25"

Mundt et al. 1991

Limb-brightened edges of a cavity.

Fridlund & Liseau 1998 HST R-band

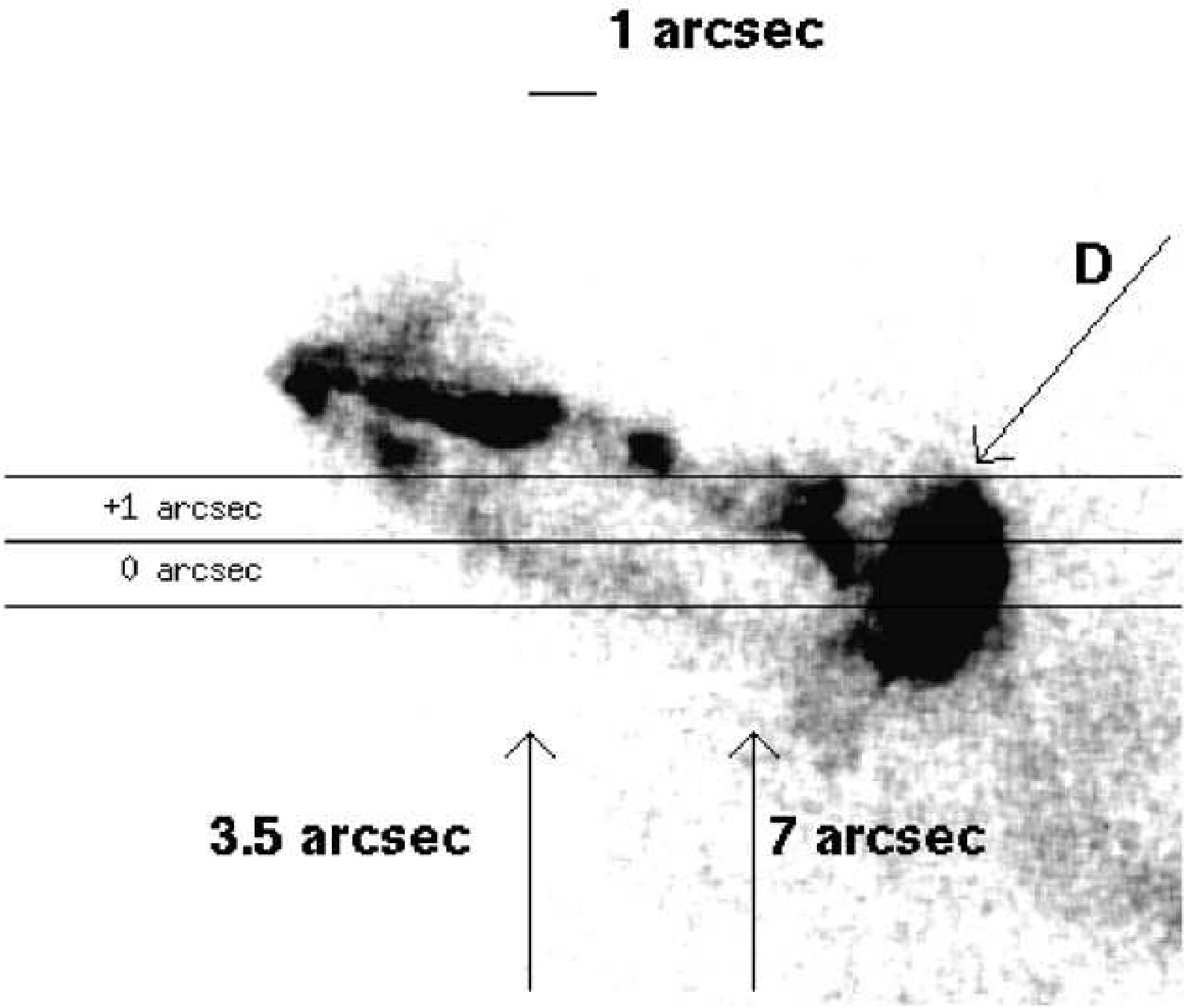

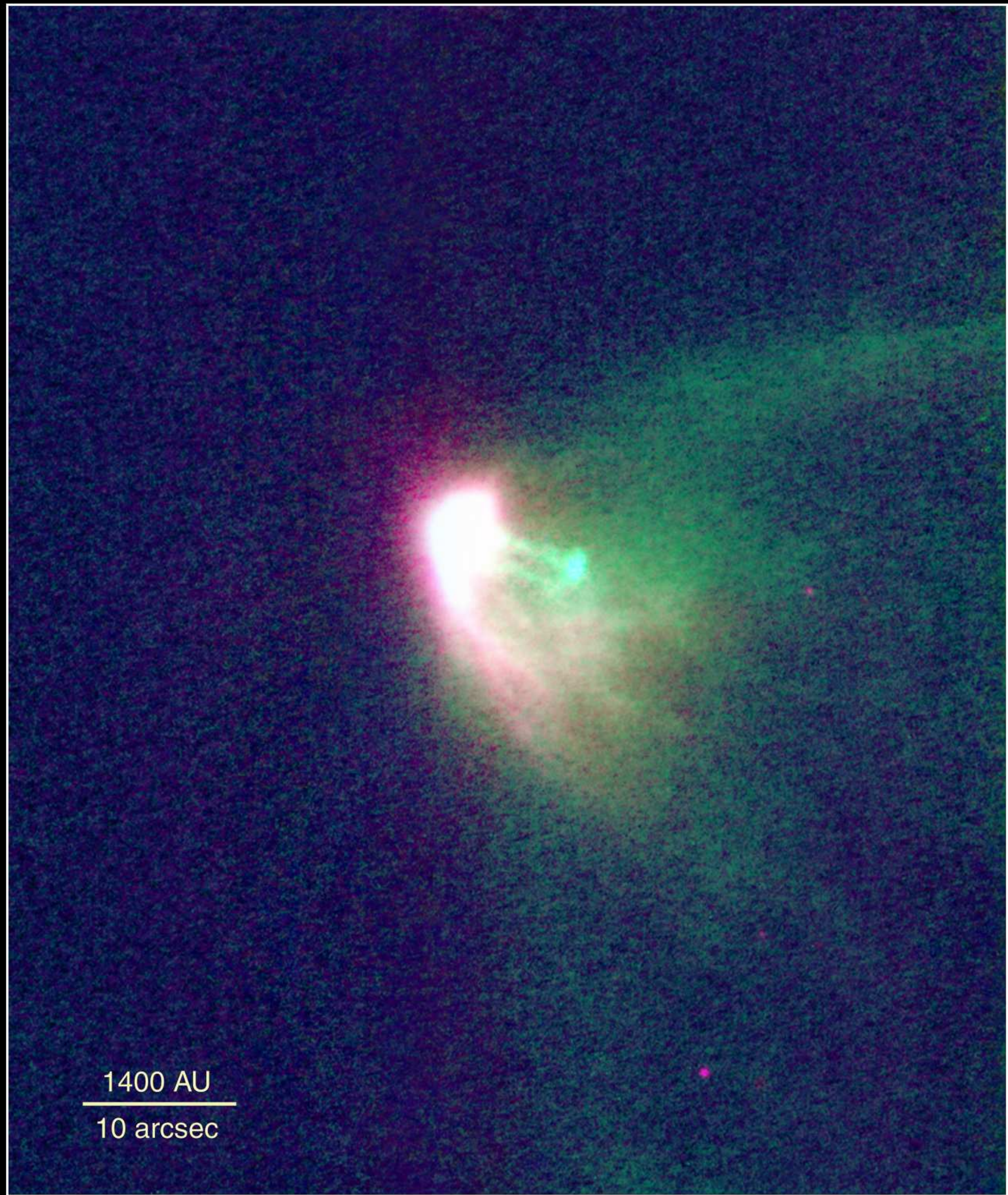

Two Jets from L1551-IRS5

Subaru Telescope, National Astronomical Observatory of Japan

CISCO (J, K′)

June 10, 1999

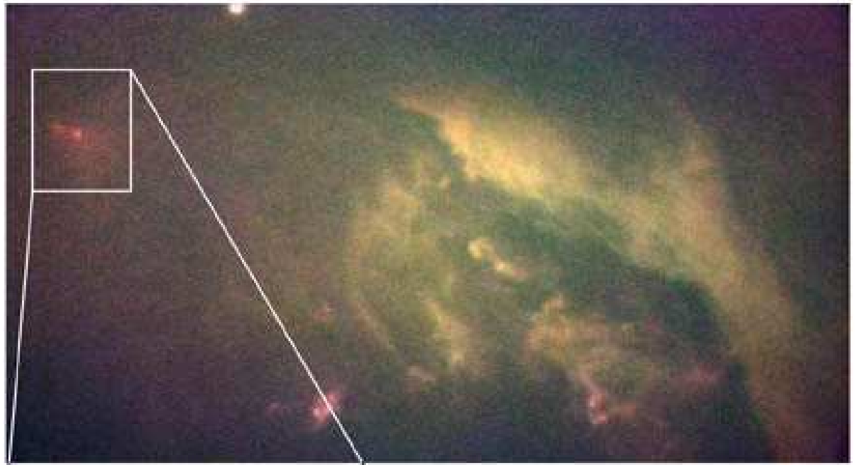

L1551-IRS5からの星風が周囲のガスと衝突して黄緑色に輝いている様子(NHKハイビジョンカメラをすばる望遠鏡に取りつけて撮影)。写っている範囲は、約6分角x3分角。
Strong wind from L1551-IRS 5 is colliding with ambient gas clouds to emit yellowish-green light (taken with the NHK HDTV Camera attached to the Subaru Telescope). The field of view is about 6 arcmin x 3 arcmin.

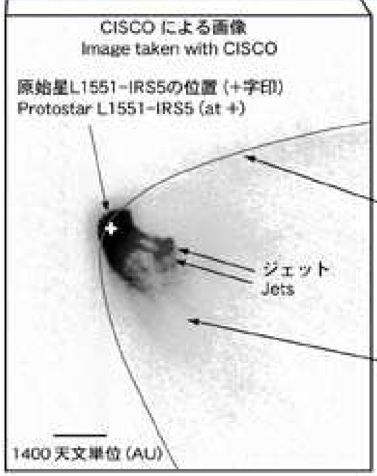

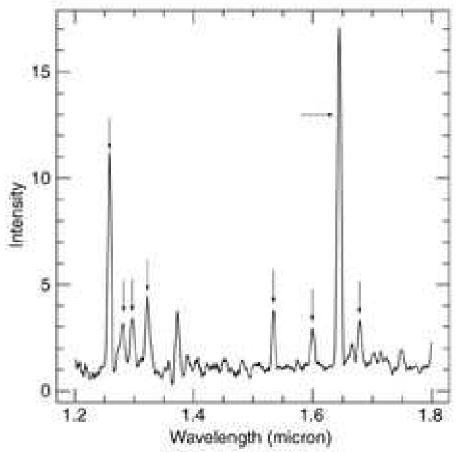

2本あるL1551-IRS5からのジェットのうち、北（上）側のジェットの根本近くのスペクトルを示した。横軸が波長で、縦軸が赤外線強度。何本かの鋭いピーク（矢印）は鉄イオンの出す輝線スペクトルであり、ジェットがほとんど鉄イオンの輝線で光っていることがわかる。このスペクトルを解析することで、ジェットの温度は数千度あり、また密度(電子の密度)が1立方センチあたり約1万個であることもわかった。

An infrared spectrum of the northern (upper) jet taken near its base. The intensity of infrared light is plotted against its wavelength. Several strong peaks (indicated by arrows) are due to emission from ionized iron; the jet is bright only in iron line emission. Analysis of this spectrum gives the temperature and density of the jet to be several thousand Kelvin and 10,000 cm^{3} respectively.

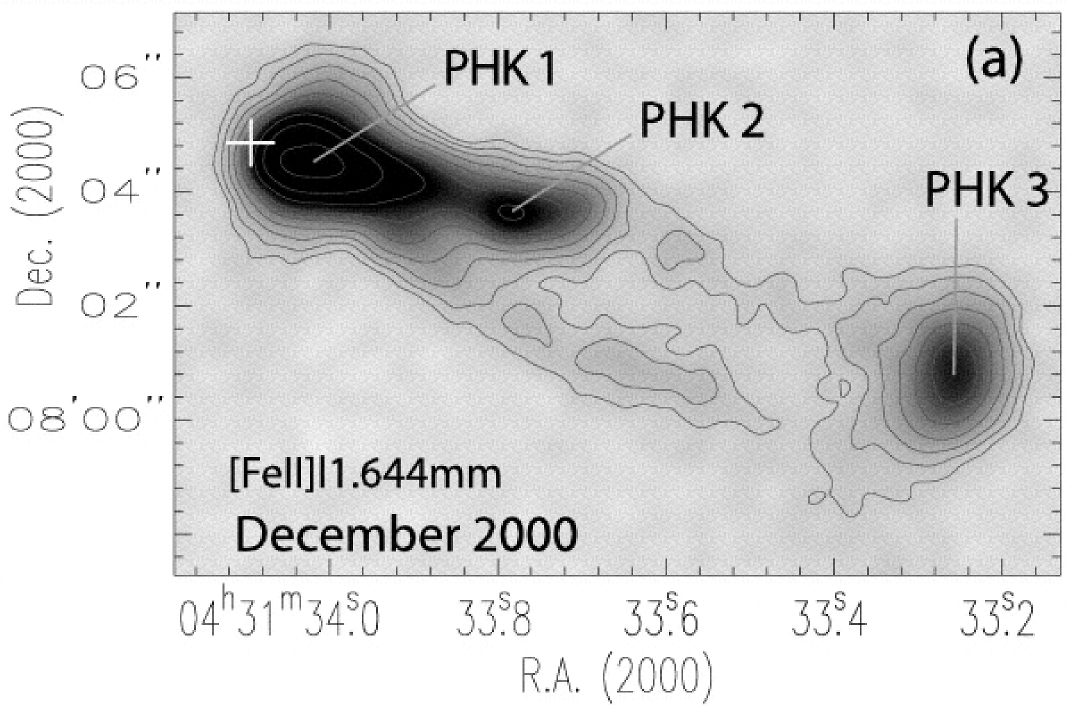

Pyo et al. 2002

SUBARU

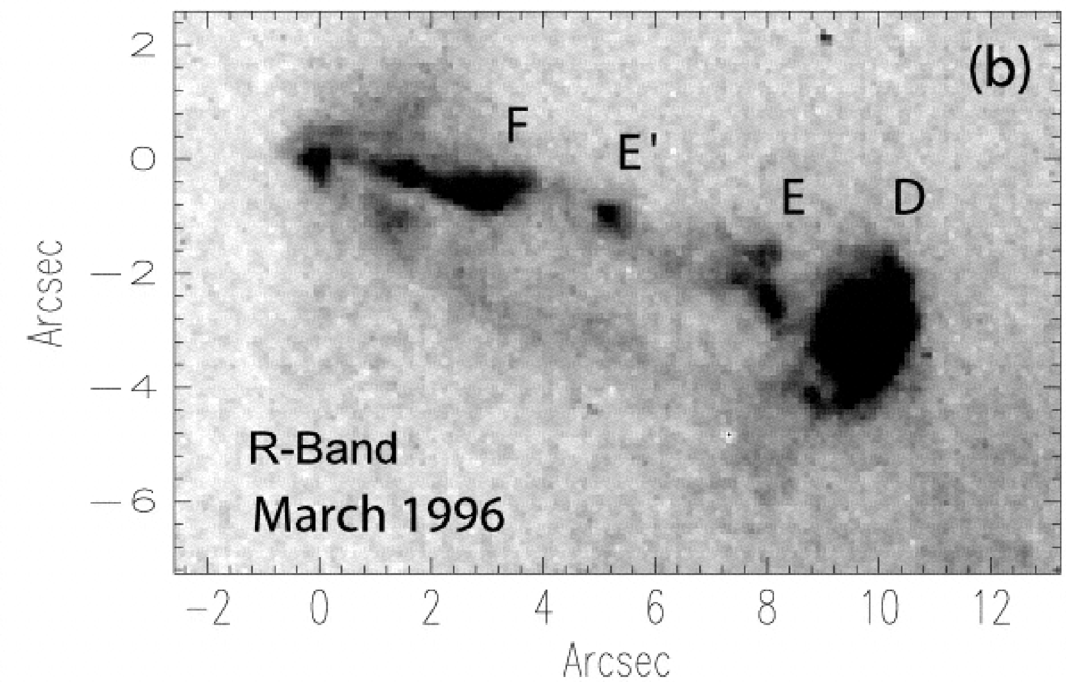

Fridlund & Liseau 1998

HST

Pyo et al. 2002

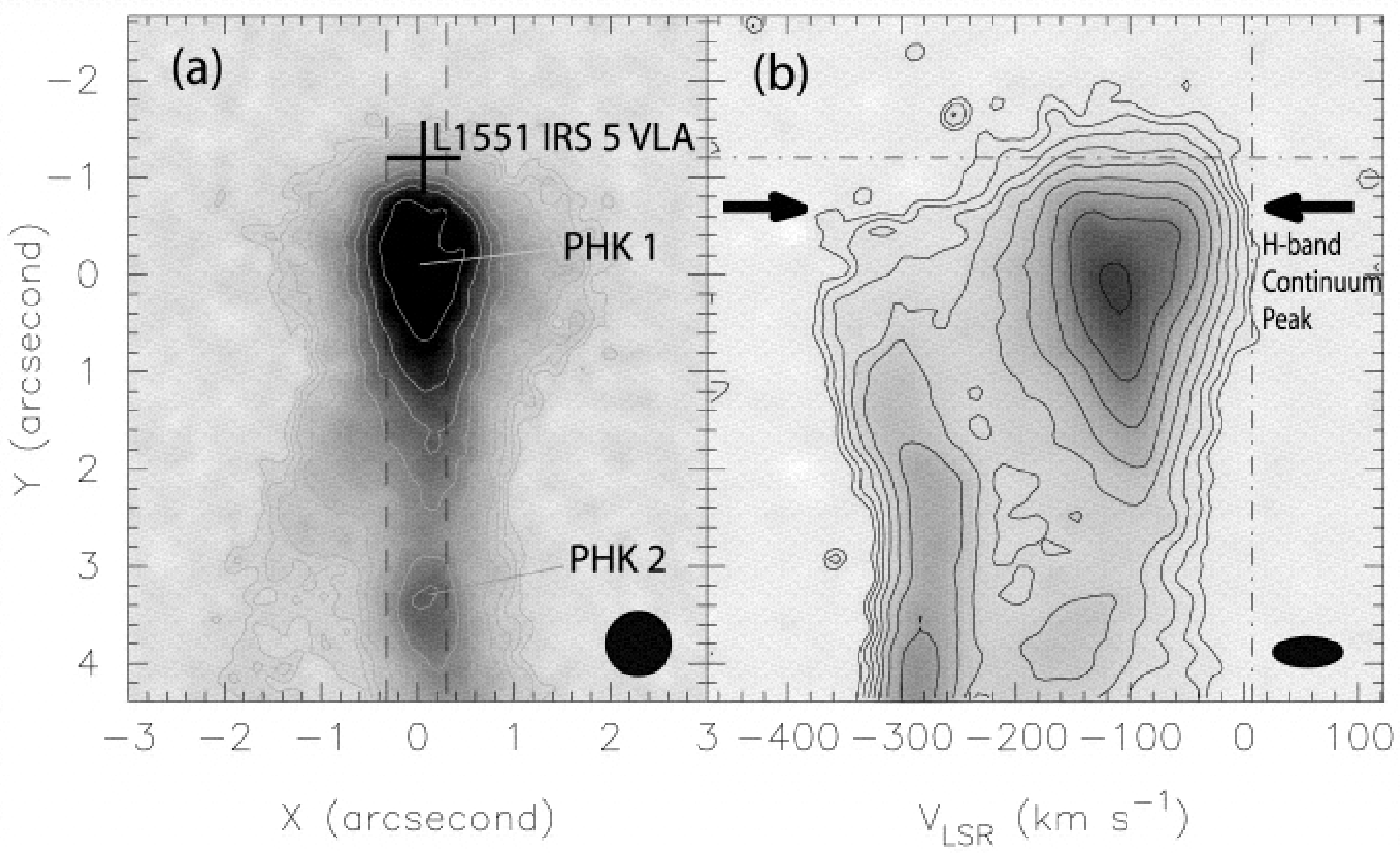


Very Large Array

Very Long Baseline Array


Pie Town antenna

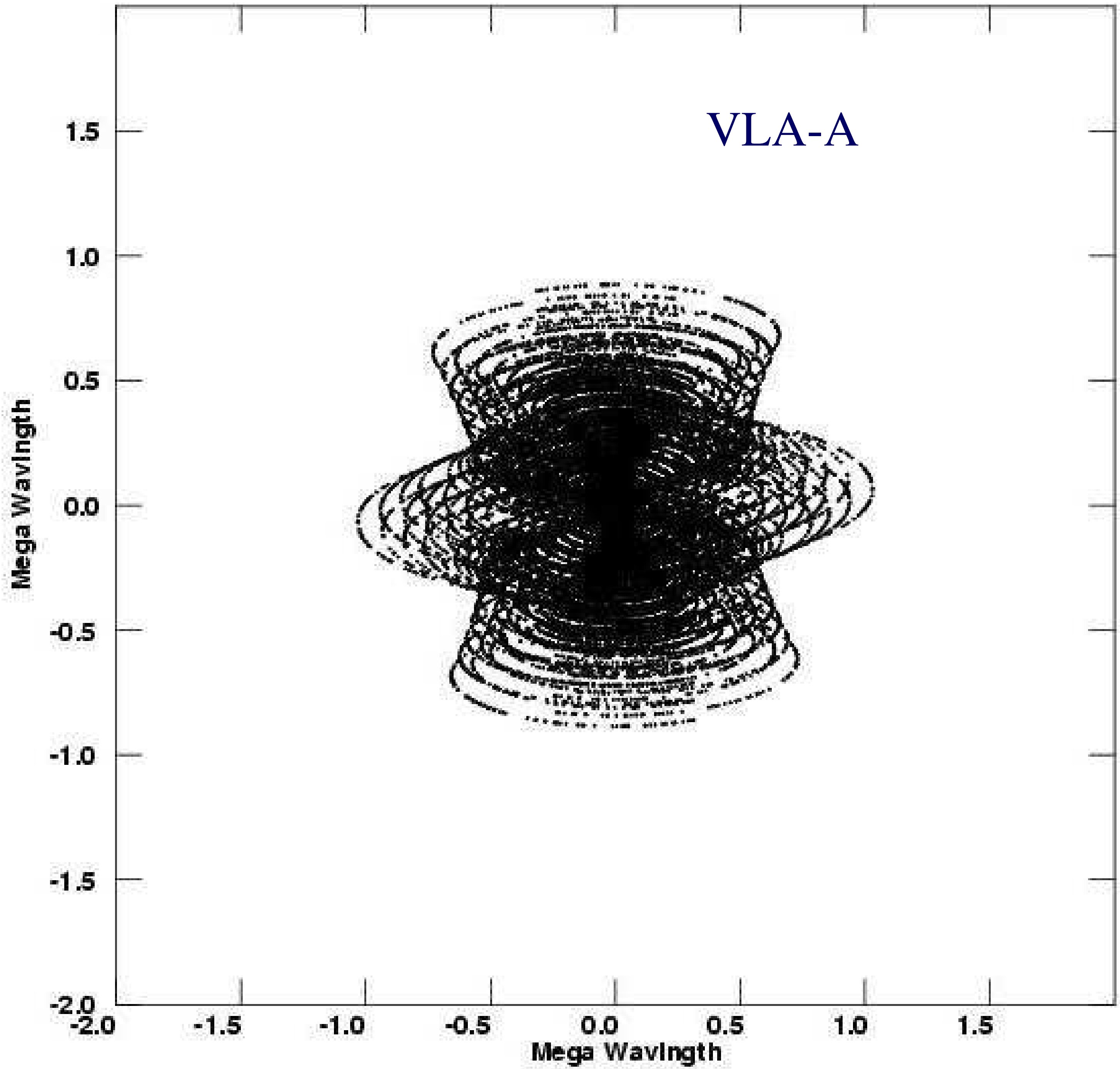
VLA-A
1.5
1.0
0.5
0.0
-0.5
-1.0
-1.5
-2.0
Mega Wavlngth
-2.0
-1.5
-1.0
-0.5
0.0
0.5
1.0
1.5
Mega Wavlngth

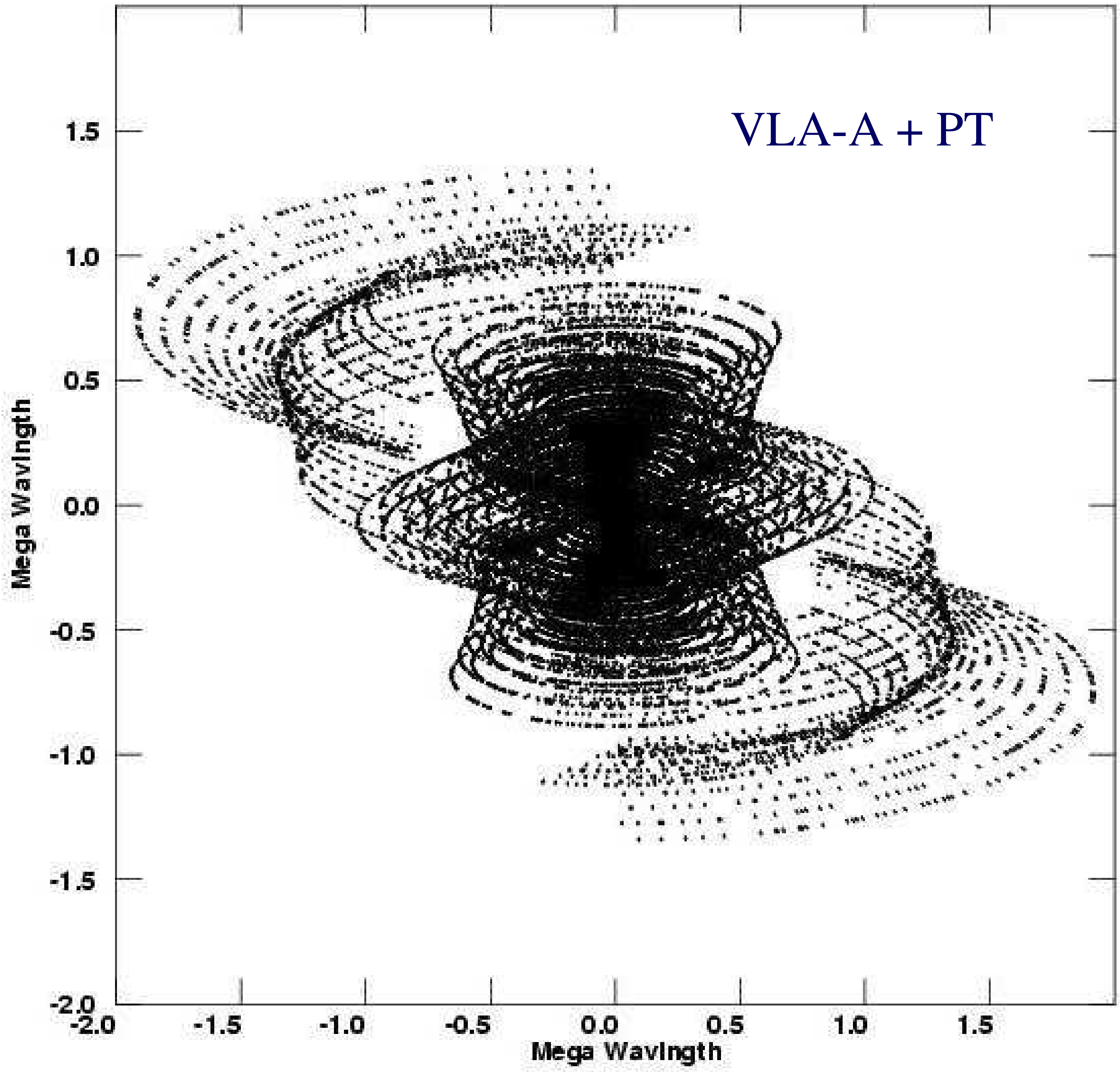

VLA-A + PT
Mega Wavlngth
Mega Wavlngth
1.5
1.0
0.5
0.0
-0.5
-1.0
-1.5
-2.0
-2.0
-1.5
-1.0
-0.5
0.0
0.5
1.0
1.5

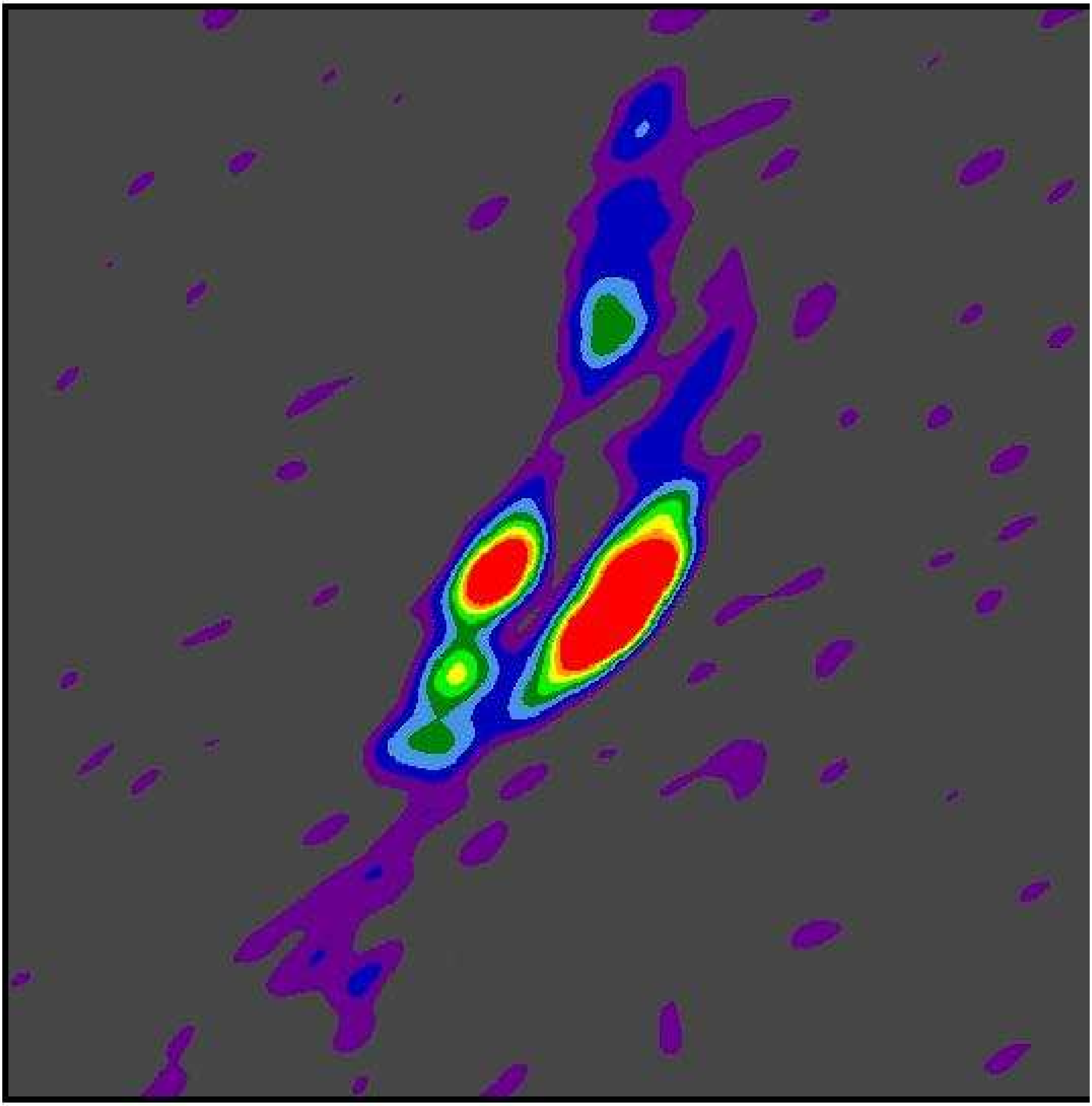

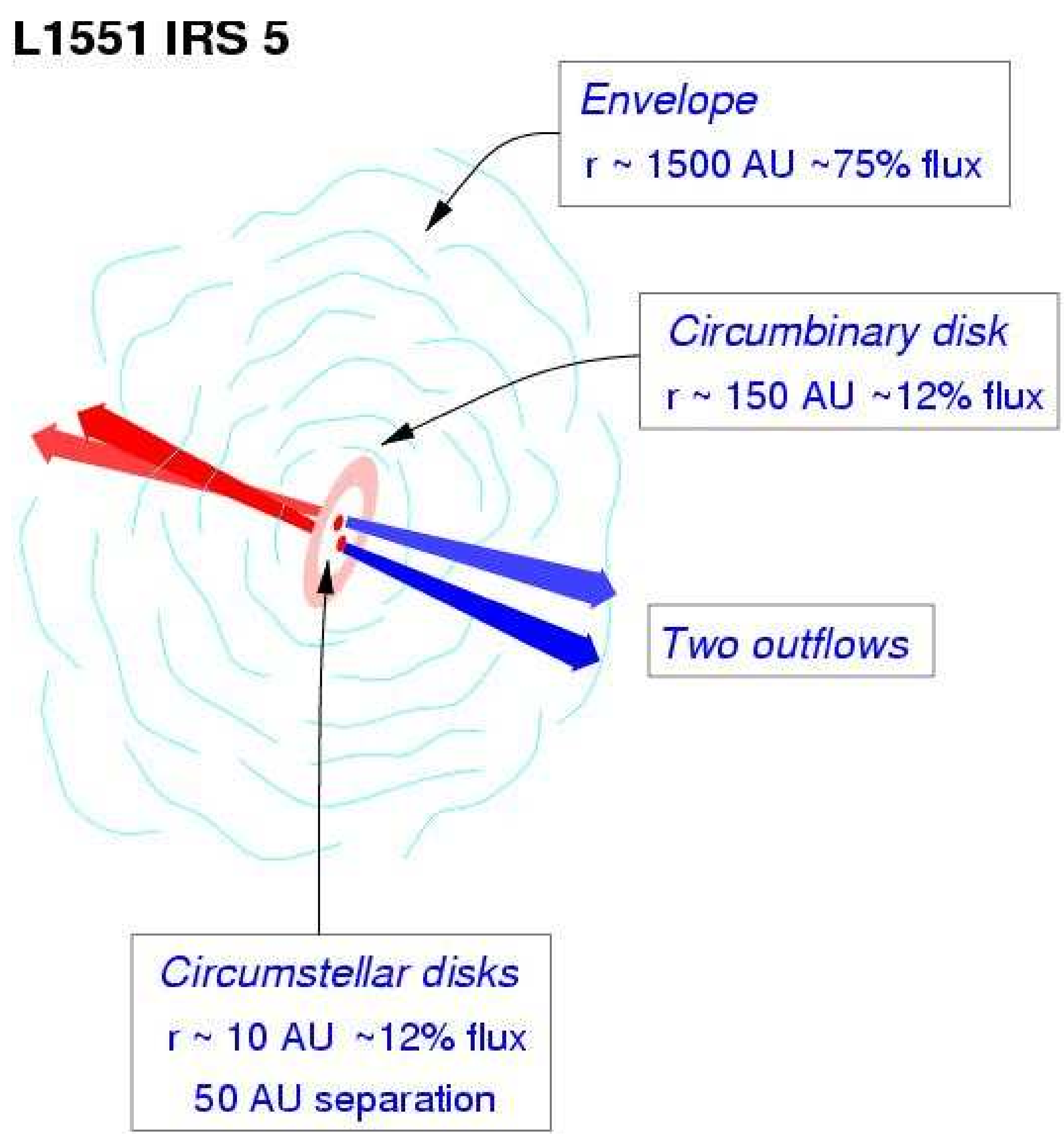
L1551 IRS 5
Envelope
r ~ 1500 AU ~75% flux
Circumbinary disk
r ~ 150 AU ~12% flux
Two outflows
Circumstellar disks
r ~ 10 AU ~12% flux
50 AU separation

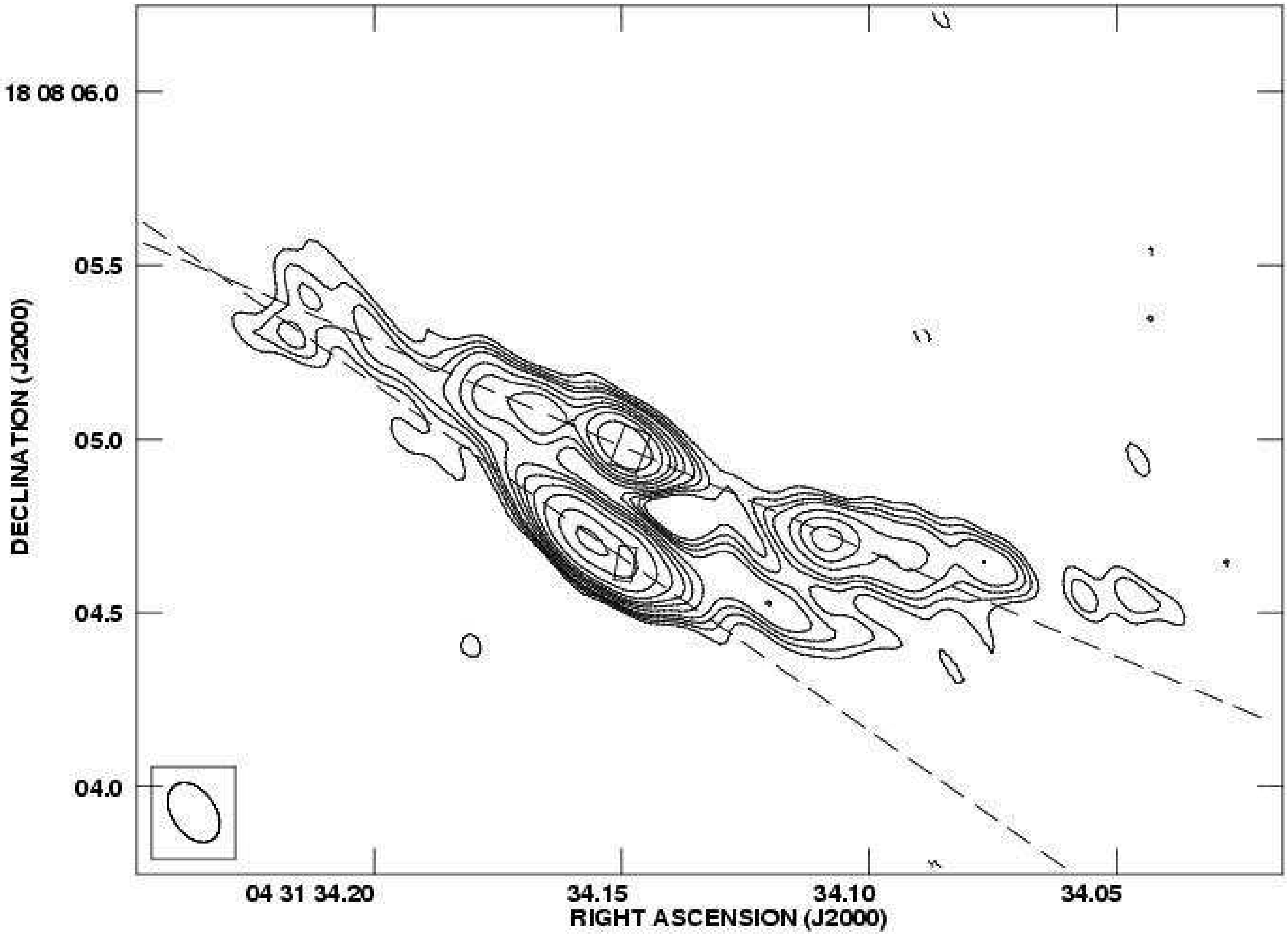

18 08 06.0
05.5
05.0
04.5
04.0
DECLINATION (J2000)
04 31 34.20
34.15
34.10
34.05
RIGHT ASCENSION (J2000)

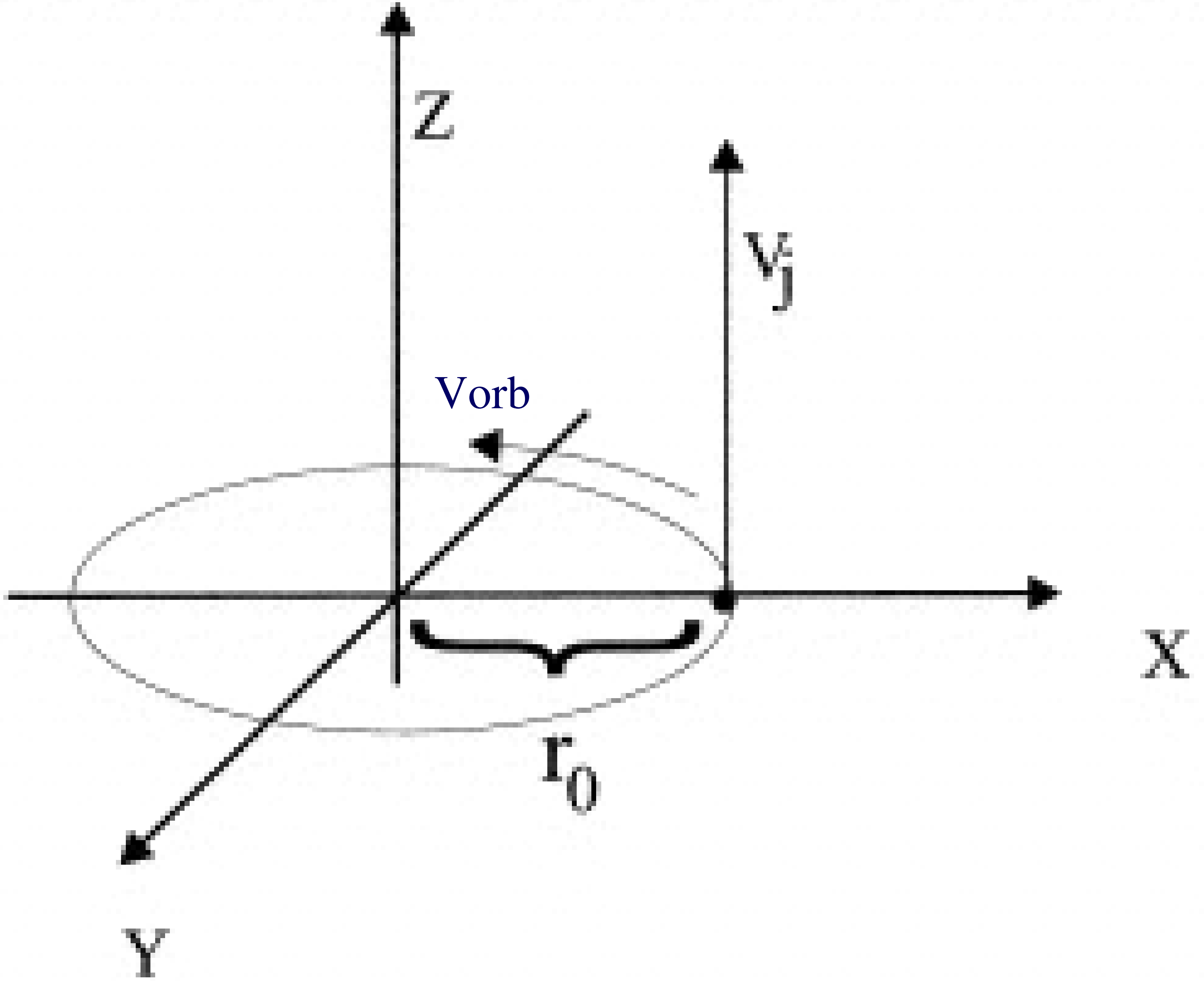
Z
V_j
Vorb
X
r_0
Y

Masciadri & Raga 2002

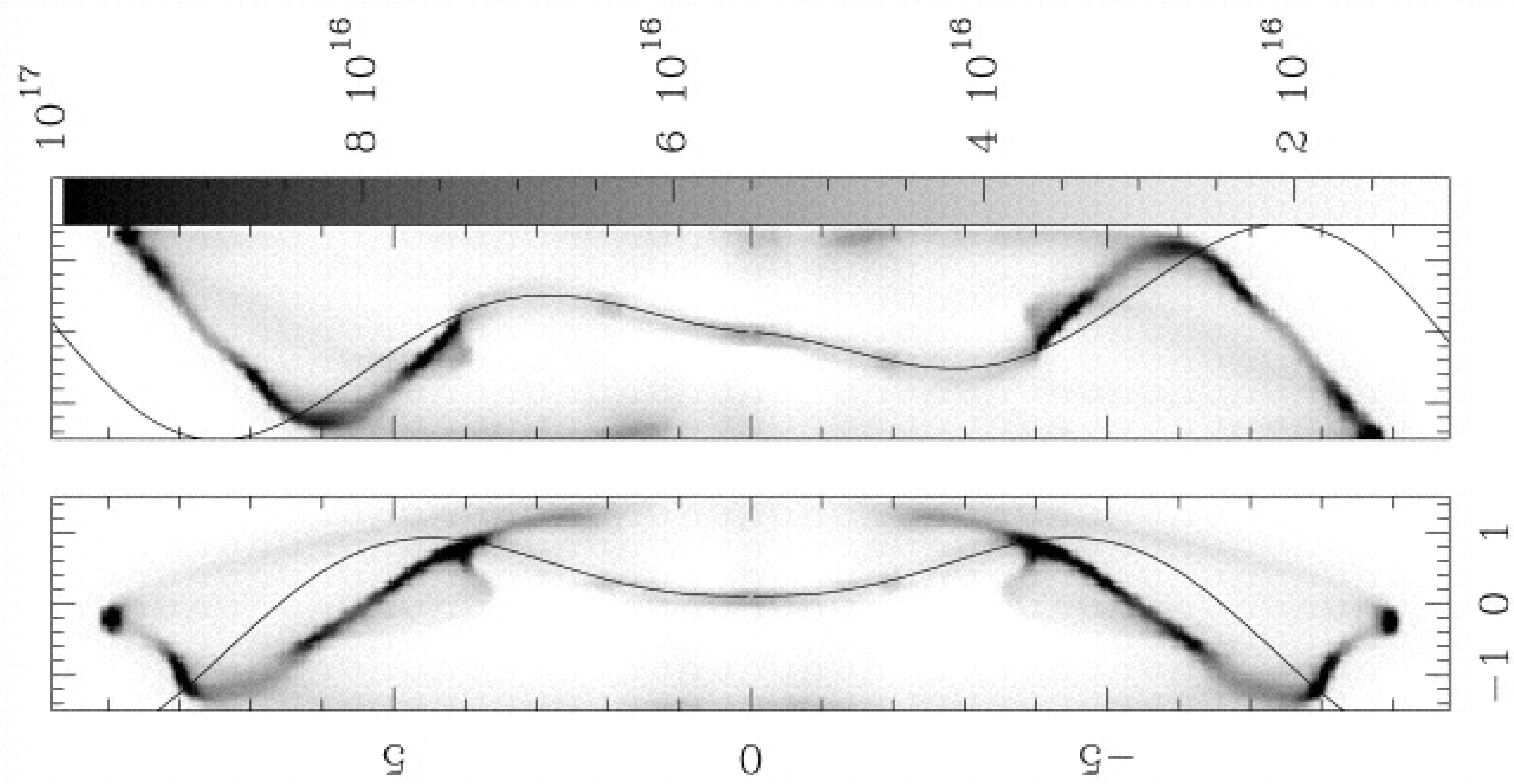

V(orbital)/V(jet) = 1/10

But V(orbital) = 5 km/s

Which appears to imply a V(jet) of only 50 km/s

Too slow for the L1551 IRS5 jets

SubMillimeter Array (SMA) in Mauna Kea, Hawaii

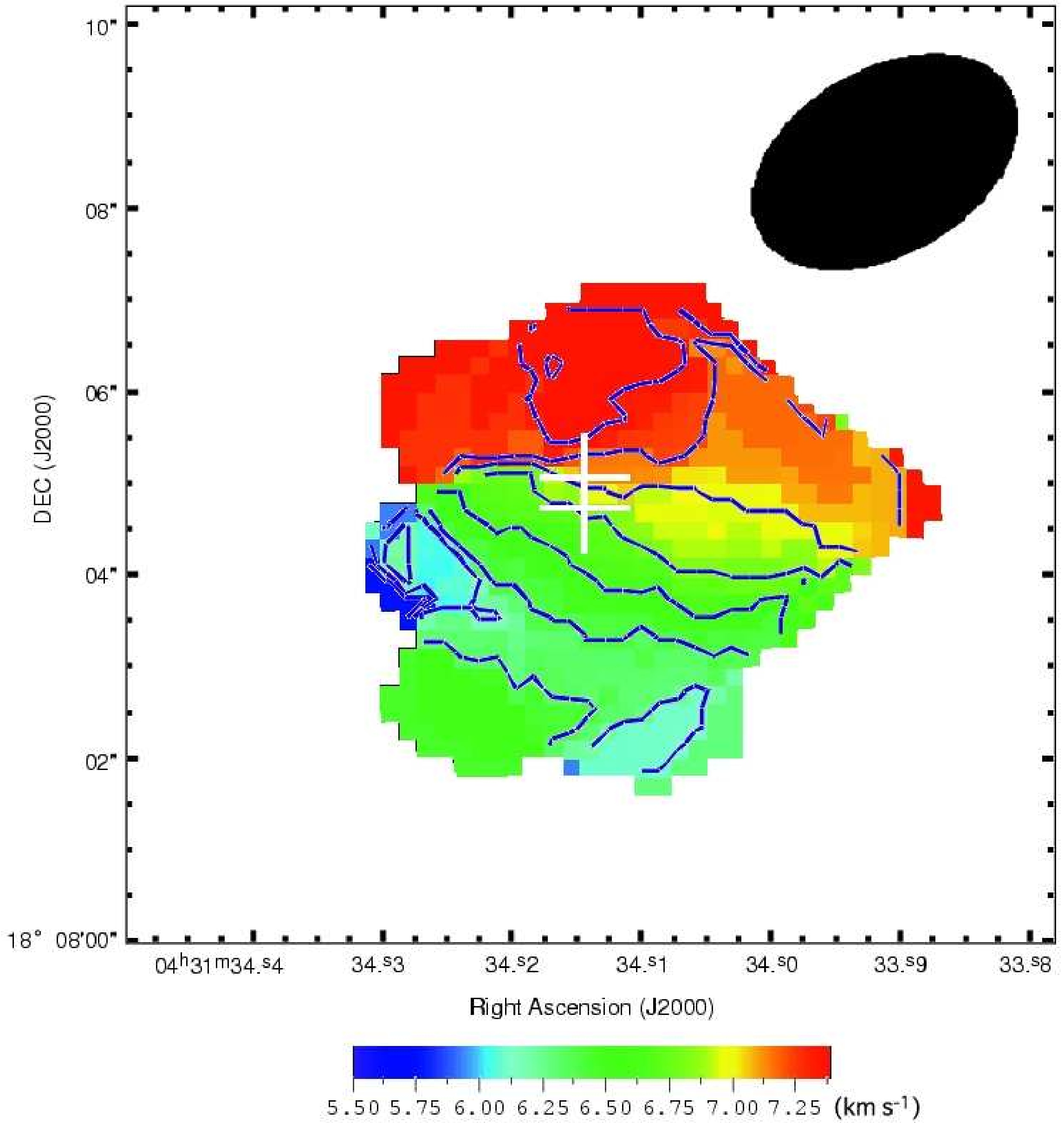

SMA observations of CS (J=7-6) line show rotating circumstellar envelope that probably feeds the disks at the center (Takakuwa et al. 2004).

Conclusions

- Two jets in L1551 IRS5. Collimation within 10 AU.
- The north jet shows “mirror” symmetry perhaps due to orbital motions.
- There is a region of emission between the jets that could be due to interaction.
- Repeat VLA+Pie Town observations to understand dynamics of jets.

Favata et al. 2002

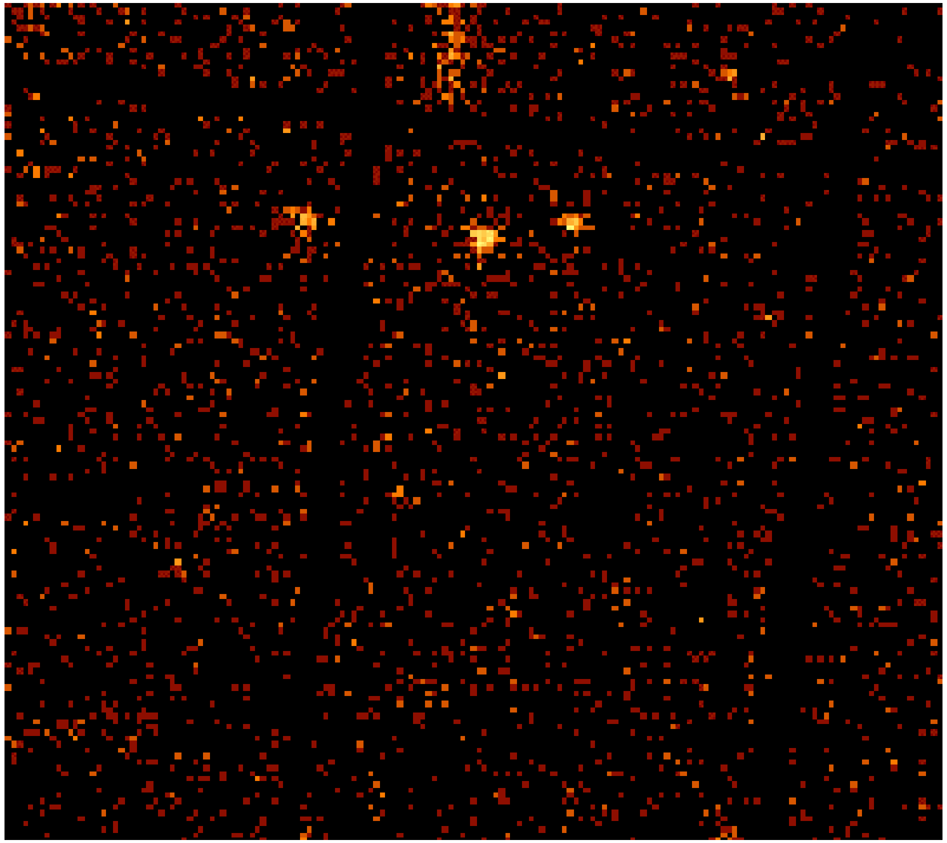

XMM 0.3-7.9 keV

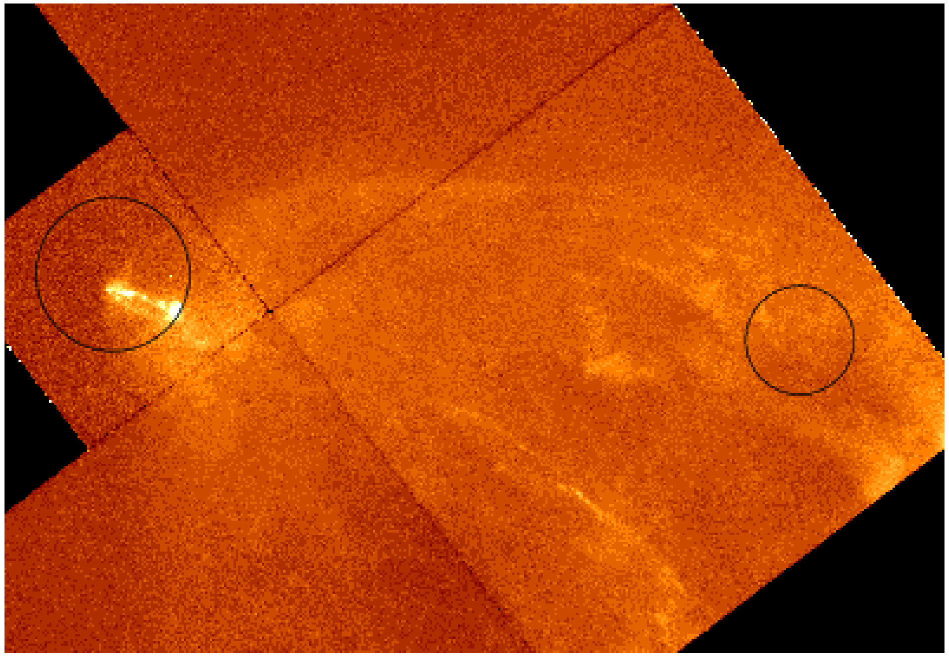

HST R-band